

AD \_\_\_\_\_

COOPERATIVE AGREEMENT NUMBER DAMD17-94-V-4013

TITLE: YopM Plague Vaccine Component: Immunogenicity,  
Protectiveness, and Mode of Action

PRINCIPAL INVESTIGATOR: Susan C. Straley, Ph.D.

CONTRACTING ORGANIZATION: University of Kentucky Research  
Foundation  
Lexington, Kentucky 40506-0056

REPORT DATE: January 1998

TYPE OF REPORT: Final

PREPARED FOR: Commander  
U.S. Army Medical Research and Materiel Command  
Fort Detrick, Frederick, Maryland 21702-5012

DISTRIBUTION STATEMENT: Approved for public release;  
distribution unlimited

The views, opinions and/or findings contained in this report are those of the author(s) and should not be construed as an official Department of the Army position, policy or decision unless so designated by other documentation.

19980410 018

DTIC QUALITY INSPECTED 3

# REPORT DOCUMENTATION PAGE

Form Approved

OMB No. 0704-0188

Public reporting burden for this collection of information is estimated to average 1 hour per response, including the time for reviewing instructions, searching existing data sources, gathering and maintaining the data needed, and completing and reviewing the collection of information. Send comments regarding this burden estimate or any other aspect of this collection of information, including suggestions for reducing this burden, to Washington Headquarters Services, Directorate for Information Operations and Reports, 1215 Jefferson Davis Highway, Suite 1204, Arlington, VA 22202-4302, and to the Office of Management and Budget, Paperwork Reduction Project (0704-0188), Washington, DC 20503.

1. AGENCY USE ONLY (Leave blank)		2. REPORT DATE January 1998	3. REPORT TYPE AND DATES COVERED Final (1 Sep 94 - 31 Dec 97)	
4. TITLE AND SUBTITLE YopM Plague Vaccine Component: Immunogenicity, Protectiveness, and Mode of Action			5. FUNDING NUMBERS DAMD17-94-V-4013	
6. AUTHOR(S)  Susan C. Straley, Ph.D.				
7. PERFORMING ORGANIZATION NAME(S) AND ADDRESS(ES)  University of Kentucky Research Foundation Lexington, Kentucky 40506-0056			8. PERFORMING ORGANIZATION REPORT NUMBER	
9. SPONSORING/MONITORING AGENCY NAME(S) AND ADDRESS(ES) Commander U.S. Army Medical Research and Materiel Command Fort Detrick, Frederick, Maryland 21702-5012			10. SPONSORING/MONITORING AGENCY REPORT NUMBER	
11. SUPPLEMENTARY NOTES				
12a. DISTRIBUTION / AVAILABILITY STATEMENT  Approved for public release; distribution unlimited			12b. DISTRIBUTION CODE	
13. ABSTRACT (Maximum 200) The plague virulence protein YopM was studied for immunogenicity, protectiveness, importance of its thrombin-binding, and its localization in infected tissue culture. YopM is highly immunogenic in mice, and human convalescent plague sera contain antibodies to YopM. However, YopM is not a good candidate for a subunit vaccine because it is not protective by either active or passive immunization. Further study is merited to determine whether diagnostic probes for <i>Yersinia pestis</i> could be based on yopM. In the cellular response to <i>Y. pestis</i> infection of naïve mice against plague, CD8 <sup>+</sup> T cells were more important than were CD4 <sup>+</sup> T cells, a finding with large implications for the pathogenesis of plague and for future efforts to improve the plague vaccine. Site-directed mutagenesis of yopM yielded mutants with normal thrombin-binding but that were as avirulent as a <i>Y. pestis</i> strain lacking YopM altogether, suggesting that thrombin-binding is not YopM's function in the pathogenesis of plague. YopM is mostly targeted into the cytosol of eukaryotic cells when <i>Y. pestis</i> adheres to them. There, YopM traffics in association with a vesicular pathway and enters the nucleus. This raises the possibility that YopM manipulates host gene expression.				
14. SUBJECT TERMS  plague, <i>Yersinia</i> , virulence protein, YopM, vaccine, thrombin, immunogenicity			15. NUMBER OF PAGES 72	
			16. PRICE CODE	
17. SECURITY CLASSIFICATION OF REPORT Unclassified	18. SECURITY CLASSIFICATION OF THIS PAGE Unclassified	19. SECURITY CLASSIFICATION OF ABSTRACT Unclassified	20. LIMITATION OF ABSTRACT Unlimited	

## FOREWORD

Opinions, interpretations, conclusions and recommendations are those of the author and are not necessarily endorsed by the U.S. Army.

\_\_\_\_ Where copyrighted material is quoted, permission has been obtained to use such material.

\_\_\_\_ Where material from documents designated for limited distribution is quoted, permission has been obtained to use the material.

SCS Citations of commercial organizations and trade names in this report do not constitute an official Department of Army endorsement or approval of the products or services of these organizations.

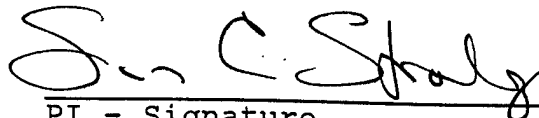
SCS In conducting research using animals, the investigator(s) adhered to the "Guide for the Care and Use of Laboratory Animals," prepared by the Committee on Care and Use of Laboratory Animals of the Institute of Laboratory Resources, National Research Council (NIH Publication No. 86-23, Revised 1985).

SCS For the protection of human subjects, the investigator(s) adhered to policies of applicable Federal Law 45 CFR 46.

SCS In conducting research utilizing recombinant DNA technology, the investigator(s) adhered to current guidelines promulgated by the National Institutes of Health.

SCS In the conduct of research utilizing recombinant DNA, the investigator(s) adhered to the NIH Guidelines for Research Involving Recombinant DNA Molecules.

SCS In the conduct of research involving hazardous organisms, the investigator(s) adhered to the CDC-NIH Guide for Biosafety in Microbiological and Biomedical Laboratories.

 1/20/98  
PI - Signature Date

## Table of Contents

Item	Pages
<u>Introduction</u>	1-2
<u>Body</u>	2-56
<u>Aim 1</u> Assess the immunogenicity and protective capacity of YopM	2-15
<u>TO 1</u> Determine if anti-YopM antibodies provide significant protection against lethal <i>Y. pestis</i> challenge	2-4
Passive protection studies	2-4
Passive immunization of mice followed by challenge with <i>Y. pestis</i> KIM5	2-4
<u>TO 2</u> Characterize the immune response in mice immunized with YopM	4-5
Immunization route and quality of humoral anti-YopM response	4-5
YopM-reactivity in convalescent plague sera	5
<u>TO 3</u> Determine if an active immune response to YopM protects mice against lethal <i>Y. pestis</i> challenge	5-15
Active immunization of mice followed by challenge with <i>Y. pestis</i> KIM5	5-7
Effect of exogenous YopM on <i>Y. pestis</i> and <i>L. monocytogenes</i> challenge in outbred mice.	7-9
Discussion of passive and active immunization findings	9-10
Roles of CD4 <sup>+</sup> and CD8 <sup>+</sup> T cells in defense against a primary infection with <i>Y. pestis</i>	11-14
Discussion of findings on relative roles of CD4 <sup>+</sup> and CD8 <sup>+</sup> T cells in defense of naïve mice against plague	15
<u>Aim 2</u> Determine if thrombin-binding is necessary for YopM function in vivo	15-36
<u>TO 1 and TO 2</u> Identify thrombin-binding sites on YopM and eliminate thrombin-binding to YopM by site-directed mutagenesis of <i>yopM</i>	15-33
Introduction	15-16
Revised sequence of YopM	16-19
Construction of mutant <i>yopM</i> genes expressing YopM proteins with defective thrombin-binding	19-25
Construction of <i>yopMS</i> and <i>yopMR</i>	19
Characterization of YopMS and YopMR	19
Results and discussion - YopMS and YopMR	20
Construction of <i>yopM</i> genes expressing internally deleted YopMs	20-25

## Table of Contents - continued

Item	Pages
General strategy	20-21
Details of the constructions	21-25
Construction of pBS15/15	21
Construction of specific deletions	22-25
Results and discussion - YopM $\Delta$ LRR proteins	25-27
<b>Platelet aggregation assay</b>	27
Results and discussion - platelet aggregation assay	27
<b>Enzyme-linked immunosorbent assay (ELISA)</b>	
<b>to quantitate YopM-human <math>\alpha</math>-thrombin binding</b>	28
Results and discussion - thrombin-binding ELISA	28
C68S and C100S YopM	29-30
Results and discussion - C68S and C100S YopM	30
Tests for which protein provides the S that crosslinks with SMCC	30-33
<b>Blocking thrombin/YopM with N-ethyl maleimide (NEM)</b>	30
Results	30
Conclusions	30-31
<b>Use of radiolabeled NEM (<math>^3</math>H-NEM) to detect blockage of -SH groups on thrombin and YopM</b>	31
Results	31
Conclusions	31
<b>Blocking of thrombin and YopM with NEM followed by crosslinking with SMCC</b>	31
Results	31
Conclusions (speculations!)	32
<b>Preincubation of YopM and thrombin-FPR followed by blockage with NEM and crosslinking with SMCC and DSS</b>	32
Results	32
Conclusion	32
Final characterization of mutant YopMs prior to testing importance of thrombin-binding in plague	32-33
<b>Test for susceptibility of YopM<math>\Delta</math>LRR4-7(4-9) and other YopM<math>\Delta</math>LRR proteins to degradation by surface protease(s) of <i>Y. pestis</i> KIM</b>	33
Results	33
Conclusion	33
<u>TO 3.</u> Analyze virulence of a yopM yopM <i>Y. pestis</i> mutant in which YopM is unable to bind thrombin.	34-36

## Table of Contents - continued

Item	Pages
Virulence test for importance of thrombin-binding in plague	34-36
Allelic replacement of <i>yopM</i> with $\Delta$ LRR4-5(4-7) <i>yopM</i> or $\Delta$ LRR7-8(7-10) <i>yopM</i> in <i>Y. pestis</i> KIM	34-35
Isolation of $\Delta$ LRR4-5(4-7) <i>yopM</i> and $\Delta$ LRR7-8(7-10) <i>yopM</i> DNA fragments from pBS15/15-based clones carried in <i>E. coli</i> XL1 Blue	34
Isolation of suicide vector pLD55 ( $Tc^R$ , <i>lacZ</i> $\alpha$ )	34
Ligation of <i>yopM</i> mutant fragments with pLD55 vector followed by transformation of <i>E. coli</i> DH5 $\alpha$ ( $\lambda$ pir) with ligation mixtures	34
Allelic exchange of mutant <i>yopM</i> fragments with intact <i>yopM</i> in pCD1 of <i>Y. pestis</i> KIM5	34-35
Results and discussion - virulence of <i>Y. pestis</i> $\Delta$ LRR <i>yopM</i> mutants in BALB/c mice	35-36
<u>AIM 3</u> Determine the fate of YopM when <i>Y. pestis</i> interacts with phagocytic cells	36-56
<u>TO 1 and 2:</u> Fate of YopM when <i>Y. pestis</i> attaches to the surface of a phagocyte and when <i>Y. pestis</i> is engulfed by a phagocyte	36-56
YopM translocation in vitro: yersiniae and antibodies	37
Vectorial YopM translocation assayed in fractionated mixed cultures	37
Results and discussion - pilot studies of YopM vectorial targeting using immunoblot as assay	38-39
<b>Yops distribution by immunoblot of fractionated infected HeLa and J774 cultures - methods</b>	40
Results and discussion - vectorial targeting of YopM assayed by immunoblot	41-43
YopM distribution by immunofluorescence staining and confocal microscopy of infected HeLa cells	43-52
<b>Methods for immunofluorescence experiments</b>	44-46
Results and discussion - YopM localization within eucaryotic cells after vectorial targeting by <i>Y. pestis</i>	47-52
YopM traffics on the cell's vesicular system	49-52
Use of digitonin to enhance visualization of YopM in the eucaryotic nucleus	53
Site-directed mutagenesis of KDEL-like sequence	53
Results and discussion - "KDEL" mutant YopM	53-54
Model for YopM's movement within eucaryotic cells	54-56
Significance of YopM's nuclear localization	56

## Table of Contents - continued

Item	Pages
<u>Conclusions</u>	57-58
<u>References</u>	58-64
<u>Publications and abstracts resulting from the studies supported by Collaborative Agreement DAMD17-94-V-4013</u>	64-65
<u>Personnel receiving pay from effort DAMD17-94-V-4013</u>	65

Final Report for Collaborative Agreement DAMD17-94-C-4041  
September 1, 1994-January 31, 1998

Introduction

This project evaluated the *Yersinia pestis* (plague) virulence protein YopM as a prospective component of a subunit plague vaccine. YopM is one of a set of proteins that are secreted into the culture medium by *Y. pestis* under conditions that are believed to mimic the contact of the bacteria with a phagocytic cell (1). At the time this Collaborative Agreement was established two of these proteins were known to be directly targeted from the bacterium into the phagocyte, with resulting paralysis of phagocytosis. The fate of YopM was not known and was investigated in this project (Aim 3). It was thought that at least some of YopM is likely to be present in the extracellular surroundings in tissues, because we had shown that YopM binds human  $\alpha$ -thrombin sufficiently tightly to prevent activation of platelets (2,3), and  $\alpha$ -thrombin is generated extracellularly by the activation of the serum protein prothrombin (4). YopM does not bind prothrombin (3); hence YopM was believed to act by sequestering thrombin as it is generated from prothrombin at foci of infection (1,3). This would be expected to have an anti-inflammatory effect, which could contribute to the virulence of *Y. pestis*, and indeed we had found that YopM is necessary for the full virulence of *Y. pestis* in mice (2). Because YopM was thought to be located extracellularly, where it would be accessible to antibody, and was necessary for full virulence of *Y. pestis*, its activity might be neutralizable by antibody, thus affording some protection against plague. This was the basic hypothesis that was being tested in the Collaborative Agreement DAMD17-94-C-4041.

The three Aims in the Collaborative Agreement examined different aspects of the hypothesis. The studies of Aim 1 generated reagents (pure YopM and antibody against YopM) that were to be used in all aims and used these reagents to characterize the immune response to YopM and to test whether mice that are actively or passively immunized against YopM are protected against plague. These studies directly asked the question of whether YopM is a protective antigen. Aim 2 determined if thrombin-binding is the main function of YopM during an infection. We made a set of mutant *yopM* genes. The YopMs expressed by these were characterized for their thrombin-binding, and two *Y. pestis* strains carrying mutant *yopMs* were tested for their virulence in mice. These tests would indicate the importance of thrombin-binding in YopM's virulence function. In Aim 3, we tested the assumption that YopM is extracellular by determining whether YopM is secreted to the medium or into phagocytes or both when *Y. pestis* contacts a macrophage. The fraction of YopM secreted to the medium would measure the relative significance of YopM's extracellular role in its virulence function. If some or all of YopM enters macrophages, then we would have learned that YopM likely has a function other than,



or in addition to, thrombin-binding. The studies of Aims 2 and 3 better characterized the mechanism of action of YopM, and the findings may be useful when considering future developmental efforts for plague vaccines and diagnostic tests.

## Body

### Aim 1. Assess the immunogenicity and protective capacity of YopM

#### Technical objective (TO) 1. Determine if anti-YopM antibodies provide significant protection against lethal *Y. pestis* challenge.

YopM to be used to immunize mice was purified and cleaned of endotoxin to < 1 ng endotoxin per mouse per immunization with End-X B52 resin (Associates of Cape Cod, Inc., Woods Hole, MA.), and mouse  $\alpha$ -YopM antibody was prepared and used for passive immunization studies (16). We provided pure YopM to Col. Friedlander's plague research group at USAMRIID in fulfillment of the YopM deliverable. We sent purified mouse anti-YopM to fulfill the antibody deliverable of this Collaborative Agreement.

Passive protection studies. We made passive protection tests using both mouse  $\alpha$ -YopM and, because this reagent was limited in amount, we provided rabbit  $\alpha$ -YopM as well as a positive control rabbit antibody against LcrV ( $\alpha$ -HTV) to this project for protection tests. We had not requested use of rabbits in this Collaborative Agreement, but we had appropriate antibodies on hand, as we had produced them for a concurrently running NIH-supported project in our lab.

Passive immunization of mice followed by challenge with *Y. pestis* KIM5. To determine if antibody alone could mediate protection against *Y. pestis* challenge, IgG from mice immunized with YopM or BSA was passively transferred to naive inbred animals. Female BALB/c mice (6-8 wk) were passively immunized intraperitoneally (IP) with a single dose of 500  $\mu$ g of mouse  $\alpha$ -YopM IgG or negative control ( $\alpha$ -BSA) IgG in 500  $\mu$ l of PF-PBS. Control mice received 500  $\mu$ l of pyrogen-free phosphate-buffered saline (PF-PBS), IP. Twenty-four hours after passive immunization, the mice were bled, and pooled serum samples tested by ELISA to determine that  $\alpha$ -YopM or  $\alpha$ -BSA antibodies had entered the serum. Forty-eight hours after immunization, groups of 10 mice were challenged intravenously (IV) via the retro-orbital sinus with decimally increasing doses of *Y. pestis* KIM5 ( $10^1$  to  $10^4$  CFU) in 100  $\mu$ l of PF-PBS. In these and all other challenge experiments, the actual CFU given were confirmed by plating. The mice were observed for 17 days after challenge, and the average doses required to kill 50% of the mice ( $LD_{50}$ ) for the treatment groups were calculated (6). Following challenge with *Y. pestis* KIM5, there were no significant differences in CFU of *Y. pestis* required to kill 50% of the animals in any of the three groups, indicating that YopM antibody on its own is not protective (Table 1). However, there appeared to be a slight

increase in the LD<sub>50</sub> values for animals immunized with antibody against bovine serum albumin ( $\alpha$ -BSA) or  $\alpha$ -YopM antibody, indicating a small non-specific protective effect of antibody per se (Table 1).

Outbred Swiss Webster mice were also examined to determine if immunization with  $\alpha$ -YopM was protective. Female Swiss-Webster mice were immunized as above with  $\alpha$ -YopM or positive control ( $\alpha$ -HTV) Ig in PF-PBS, while control mice were given PF-PBS. Twenty-four hours later, they were assessed for  $\alpha$ -YopM and  $\alpha$ -HTV antibody as above. Forty-eight hours after immunization, groups of 5 mice were challenged IV with 10<sup>1</sup> to 10<sup>5</sup> CFU of *Y. pestis* KIM5, observed for 14 days, and LD<sub>50</sub> values were determined. However, the presence of  $\alpha$ -YopM antibody also did not increase the LD<sub>50</sub> value in these passively immunized mice when compared to control animals (Table 1). Interestingly, 60% of mice given  $\alpha$ -HTV antibody were protected at a challenge dose of 10<sup>4</sup>, while all mice at this same dose in the two other treatment groups had died by day 7 post-challenge (data not shown), indicating that antibody against LcrV is protective as previously shown (8) and showing that mice can be protected against experimental plague by our immunization protocol.

These data show that YopM is not protective by passive immunization and will be discussed further below along with the results of active immunization tests.

**Table 1. Passive immunization of BALB/c and Swiss Webster mice followed by challenge with *Y. pestis* KIM5.**

Mouse Strain	Immunogen	$\mu$ g IgG per mouse	YopM Serum Antibody Titer	LcrV Serum Antibody Titer	LD <sub>50</sub> value (CFU/mouse)
BALB/c	PBS	0	$\leq 10^1$	Nd <sup>a</sup>	$4.5 \times 10^1$
	anti-BSA <sup>b</sup> IgG	500	$\leq 10^1$	ND	$2.6 \times 10^2$
	anti-YopM <sup>b</sup> IgG	500	$10^4$	ND	$3.0 \times 10^2$
Swiss-Webster	PBS	0	$\leq 10^1$	$\leq 10^1$	$1.5 \times 10^1$
	anti-HTV <sup>c</sup> IgG	500	$\leq 10^1$	$10^4$	$> 1.0 \times 10^4$
	anti-YopM <sup>c</sup> IgG	500	$10^4$	$\leq 10^1$	$< 1.0 \times 10^1$

<sup>a</sup> ND - not determined

<sup>b</sup> mouse Ig

<sup>c</sup> rabbit Ig

## TO 2. Characterize the immune response in mice immunized with YopM

Immunization route and quality of humoral anti-YopM response. We determined the optimum adjuvant (Freund's [FA]), route of administration of antigen (IP), timecourse of the antibody response (maximal by 15 d), and character of the antibody response to YopM (i.e., amounts of  $\alpha$ -YopM isotypes and subclasses) for active immunization of mice with pure YopM.

IP and subcutaneous (SC) immunization produced the highest titers, probably because FA was used. At bleed #2, the anti-YopM titer for the SC route was 10-fold lower than for IP, but by bleed #3, the titers were comparable. We concluded that we should use either IP or SC immunization for experiments that aim to test whether active immunization with YopM can be protective. It was beyond the scope of this project to attempt to mimic in mice the exact route and adjuvant combination that might be used in humans. It made sense to use a more central (IP) than peripheral (SC) immunization route for our particular plague model, as we must challenge intravenously (IV) with *Y. pestis* KIM. As expected (12), the predominant antibody type elicited was IgG1, and this was true for all routes tested. This also is the predominant serum antibody type in humans (12). It was not expected that there would be much IgM in hyperimmunized animals; nor did we anticipate that there would be a significant IgA titer, as a

mucosal immune response would not have been significantly stimulated by any of the routes.

YopM-reactivity in convalescent plague sera. We did one additional experiment that falls under the classification of characterization of the humoral response to YopM. By way of relating our study more directly to its potential relevance for humans, we determined if three samples of human plague convalescent serum, known by a standard passive hemagglutination test to have specific reactivity for the capsular protein F1, would also have reactivity for YopM and LcrV. Many years ago, we had obtained three samples of human convalescent plague serum from T. Quan (Centers for Disease Control and Prevention, Ft. Collins, CO). Their sample designations and passive hemagglutination (pHA) titers (9, 10) against *Y. pestis* capsular antigen (fraction 1 antigen) were: TX84-220, pHA 1:32 ; 80NM 912, pHA 1:512; 77NM 697C, pHA 1:32. These sera were tested for YopM and LcrV serum antibody titers using an indirect ELISA method (16).

All of the samples had reactivity against YopM (titers 1:800-1:1600 by ELISA) and LcrV (titers 1:1600 to  $\geq$ 1:3200 by ELISA). The serum sample with the highest agglutination titer to F1 (1:512) also had the highest Ab titer to LcrV ( $\geq$  1:3200 [highest dilution tested]) but had a lower titer to YopM (1:800). In contrast, the serum sample with the highest titer to YopM (1:1600) had a relatively lower titer to LcrV (1:1600) and a low agglutination titer to F1 (1:32). Accordingly, as with the known protective antigens F1 and V antigen, YopM also is expressed sufficiently during human plague to elicit a specific immune response. We speculate that YopM is sufficiently present in infection of humans to exert its virulence effects.

### TO 3. Determine if an active immune response to YopM protects mice against lethal *Y. pestis* challenge.

We tested the protective efficacy of active immunization, as this protocol might prime effector cells which may be required in addition to YopM-specific antibody to protect against *Y. pestis* challenge. We used HTV as a positive control, protective antigen in some tests. Its purity was estimated by SDS-PAGE on a 12.5% (wt/vol) gel followed by silver staining. Endotoxin concentrations were confirmed by limulus amoebocyte lysate (LAL) assay (BioWhittaker Inc., Walkersville, MD) to be  $\leq$  1ng per 40  $\mu$ g of protein.

### Active immunization of mice followed by challenge with *Y. pestis* KIM5.

For challenge with *Y. pestis*, female, 8-week old BALB/c mice were immunized IP biweekly for 6 weeks with 0.2 ml containing 40  $\mu$ g of YopM in PF-PBS emulsified 1:1 with FA or PF-PBS + FA alone (control mice). Unless otherwise specified, titers of relevant antibodies (here,  $\alpha$ -YopM) were assessed in active immunization experiments by ELISA 24 h before each immunization and 1 d before challenge. Eighteen days after the third and final boost, groups of 5 mice were challenged IV with decimally increasing doses ( $10^1$  to  $10^7$  CFU) of *Y. pestis* KIM5 in 100  $\mu$ l of PF-PBS. The mice were observed for 24 days post-challenge,

and LD<sub>50</sub> values were determined. In this first study, the  $\alpha$ -YopM antibody titer in pooled serum from immunized BALB/c mice was 10<sup>5</sup> by ELISA at the time of challenge. In PBS-treated mice the  $\alpha$ -YopM antibody titer was <10<sup>2</sup> (lowest dilution tested) in pooled sera. In both treatment groups mice began to die 2 days post-challenge with the highest challenge dose. The LD<sub>50</sub> in the YopM immunized group of mice was not significantly different from that of the PBS-treated group following challenge with *Y. pestis* KIM5 (Table 2), indicating that YopM is not a protective antigen.

We were concerned that the high dose of YopM given for immunization might not have been completely eliminated by the mice by 18 d after the final boost (at time of challenge) and might have had a residual effect on host defenses at challenge. Accordingly, we modified the immunization protocol to give a smaller amount of YopM immunogen with only one boost and a longer time period (1 month) between the last immunization and challenge. Specifically, 6-8 week-old female BALB/c mice were immunized biweekly twice with a reduced amount of YopM (20 $\mu$ g) in PF-PBS + FA. Negative control mice received PF-PBS + FA or PF-PBS alone. Groups of 10 mice in each of the treatment categories were challenged IV with 10<sup>1</sup> to 10<sup>7</sup> CFU of *Y. pestis* KIM5 one month after the second immunization. The mice were observed for 24 days post-challenge, and LD<sub>50</sub> values were determined. As with the first study, the  $\alpha$ -YopM titers were  $\geq 10^5$  in pooled immune mouse serum and < 10<sup>1</sup> in control mouse serum. Upon challenge there was no significant difference in the LD<sub>50</sub> value when immunized and control mice were compared (Table 2), again supporting the finding that active immunization with YopM is not protective. Freund's adjuvant had a slight non-specific protective effect (Table 2).

Because BALB/c mice as a group possess only one allotype (H-2<sup>d</sup>) of the major histocompatibility (MHC class II) locus required for antigen presentation (7), they are limited in their repertoire of presentable peptides and may not effectively present YopM peptide fragments to immune effector cells. Therefore, we immunized and challenged outbred mice (Swiss-Webster), which as a group would possess a spectrum of MHC loci and thus be able to present a wider variety of peptides to effector cells. Female 6-8 week-old Swiss-Webster mice were immunized IP biweekly twice with 20  $\mu$ g of YopM + FA or HTV + FA; negative control mice were given PF-PBS + FA. Serum  $\alpha$ -YopM and  $\alpha$ -HTV titers were quantitated two weeks after the second immunization. One month after the second immunization, groups of 5 mice were challenged IV with 10<sup>1</sup> to 10<sup>5</sup> CFU of *Y. pestis* KIM5. The mice were observed for 17 days post-challenge, and LD<sub>50</sub> values were determined. Before challenge, YopM-immunized mice collectively had a specific serum antibody titer of 10<sup>5</sup> while control mice had  $\alpha$ -YopM titers of < 10<sup>1</sup>. HTV-immunized animals had a pooled  $\alpha$ -HTV serum antibody titer of > 10<sup>5</sup>, while pooled serum samples from the two other groups of mice had titers < 10<sup>1</sup>. Similar to the findings with

BALB/c mice, active immunization with YopM did not significantly increase the LD<sub>50</sub> values for these mice over those

**Table 2.** Active immunization of BALB/c and Swiss Webster mice followed by challenge with *Y. pestis* KIM5.

Mouse Strain	Expt. No.	Immunogen	µg immunogen /mouse <sup>a</sup>	YopM Serum Antibody Titer	LcrV Serum Antibody Titer	LD <sub>50</sub> value (CFU/mouse)
BALB/c	1	PBS + FA	n.a.	$\leq 10^1$	n.a.	$4.5 \times 10^3$ <sup>b</sup>
		YopM + FA	40	$10^5$	n.a.	$1.4 \times 10^3$ <sup>b</sup>
	2	PBS	n.a.	$\leq 10^1$	n.a.	$< 1.0 \times 10^1$
		PBS + FA	n.a.	$\leq 10^1$	n.a.	$1.0 \times 10^1$
		YopM + FA	20	$10^5$	n.a.	$1.2 \times 10^1$
Swiss-Webster	1	PBS + FA	n.a.	$\leq 10^1$	$\leq 10^1$	$< 1.0 \times 10^1$
		YopM + FA	20	$10^5$	$\leq 10^1$	$3.0 \times 10^1$
		HTV + FA	20	$\leq 10^1$	$\geq 10^5$	$> 1.0 \times 10^5$

<sup>a</sup> n.a. - not applicable

<sup>b</sup> The LD<sub>50</sub> values for this experiment were larger than for others with BALB/c mice, probably because the mice were older at the start of the experiment and then went through a more prolonged immunization than in other experiments.

for controls (Table 2). Mice immunized with HTV demonstrated a significant degree of resistance to challenge, as all mice survived even the highest challenge dose, indicating, as previously shown (12,13,14), that LcrV is a protective antigen.

Effect of exogenous YopM on *Y. pestis* and *L. monocytogenes* challenge in outbred mice. Because it was conceivable that YopM could have an extracellular anti-host role without being neutralizable by antibody, we tested whether exogenously supplied YopM exacerbated infections by homologous (*Yersinia*) and heterologous (*Listeria*) pathogens. Because only a few *Y. pestis* KIM5 bacteria kill mice (tables 1 and 2), we would not expect to measure reliably an exacerbating effect of YopM treatment on infection by this strain. Accordingly, we used the YopM *Y. pestis* KIM5-3233, previously shown to be attenuated in BALB/c

mice (2) and tested for the ability of exogenous YopM to reconstitute virulence.

On day 1, groups of 10 female 5-6 week Swiss Webster mice were challenged IV via the retro-orbital sinus with  $10^1$  to  $10^4$  CFU of *Y. pestis* KIM5-3233, or  $10^1$  to  $10^4$  CFU of *L. monocytogenes* EGD in 100  $\mu$ l of PF-PBS. Approximately 2 h later, 5 mice for each challenge dose were administered PF-PBS and the other 5 mice received 100  $\mu$ g YopM in 100  $\mu$ l of PF-PBS, given in the other eye. On d 2 the YopM-supplemented mice received YopM IV while on days 3, 4, 5, and 6 post-infection, they received IP injections of 100  $\mu$ g of YopM in 100  $\mu$ l of PF-PBS. This test was made twice with similar results, once using YopM not cleaned of endotoxin; the data shown in Table 3 are for endotoxin-free YopM.

To assess the effect of antibody on the action of exogenous YopM, 40 mice were injected IP with 500  $\mu$ g of rabbit  $\alpha$ -YopM antibody or irrelevant rabbit antibody (from pre-immune serum) on days 0 and 2. On day 0, ca. 4 h after receiving the antibody, groups of 10 mice were challenged retro-orbitally with  $10^1$  to  $10^4$  CFU of *Y. pestis* KIM5-3233 and then were given YopM or PBS in the other eye as above. On day 2, both YopM and antibody were administered IP. To minimize interaction of YopM and antibody in the peritoneum these proteins were administered 6h apart. Additional groups of 5 control mice were given either PF-PBS or YopM but were not challenged. The LD<sub>50</sub> and MTD values for each treatment group was determined.

YopM treatment did not exacerbate a *Listeria* infection (Table 3). However, YopM did enhance the virulence of by the YopM<sup>-</sup> *Y. pestis*, causing a more than 3-fold decrease in the LD<sub>50</sub>. This effect was swamped out by the nonspecific protective effect of large doses of any antibody (also see Table 1), so we were not able to determine whether anti-YopM antibody can neutralize exogenous YopM's virulence-enhancing effect. These findings indicate that YopM does not act by itself to counteract host defenses important for resistance to *Listeria* but that exogenously supplied YopM might have a virulence-promoting effect on *Yersinia*. This raises the possibility that YopM might have an extracellular function.

**Table 3. Effect of exogenous YopM on virulence of *Y. pestis* and *L. monocytogenes*.**

Bacterium	Exogenous YopM <sup>a</sup>	Antibody <sup>b</sup>	MTD <sup>c</sup>	LD <sub>50</sub>
<i>Y. pestis</i> KIM5-3233 <sup>d</sup>	-	none	6	7 x 10 <sup>2</sup>
	+	none	5 <sup>e</sup>	2 x 10 <sup>2</sup>
	+	anti-YopM	6	5 x 10 <sup>2</sup>
	+	irrelevant	-	3 x 10 <sup>3</sup>
<i>L. monocytogenes</i> EGD	-	none	3	3 x 10 <sup>2</sup>
	+	none	3	5 x 10 <sup>2</sup>

<sup>a</sup> 100 µg of YopM were administered (IV or IP) in 100 µl of PF-PBS on days 0 through 5.

<sup>b</sup> 500 µg of protein A-purified rabbit antibody was administered IP in 500 µl of PF-PBS on days 0 and 2. Irrelevant antibody was purified from pre-immune serum samples.

<sup>c</sup> MTD - mean time to death (days) for mice given the dose that was at least 10-fold above the calculated LD<sub>50</sub> (10<sup>4</sup> bacteria).

<sup>d</sup> *Y. pestis* KIM5-3233 is a YopM<sup>-</sup> mutant.

<sup>e</sup> Not different at 95% confidence from MTD for *Y. pestis* KIM5-3233 without exogenous YopM

#### Discussion of passive and active immunization findings.

In these experiments we sought to determine if immunization against YopM is protective against challenge with *Y. pestis*. Antibodies to YopM were hypothesized to be protective, because YopM has an in-vitro activity, thrombin-binding, that is compatible with an extracellular location for the protein during an infection and because YopM is necessary for full virulence in mice (2). Hence, antibody might have access to YopM in vivo and be able to neutralize its activity. To test our hypothesis, we used an intravenous challenge mouse model of systemic *Y. pestis* infection.

We found that YopM is highly immunogenic in mice and rabbits, and the tests with human convalescent sera indicate that humans also will respond to YopM produced during an infection with an antibody response.

However, neither passive immunization of mice with antibody from YopM-immunized mice or rabbits nor active immunization with YopM protected against *Y. pestis* challenge. In contrast, we found that both passive and active immunization against LcrV



(HTV) was protective in our mouse plague model. As seen previously, active immunization against LcrV appeared to convey strong protection (12,13,14), while passive immunization conveyed only partial protection (8), indicating that specific host factors, in addition to antibody, are required for full protection against *Y. pestis* challenge in mice.

It is possible that YopM is not neutralized by antibody because its main target in the host is intracellular. In vivo, YopM might enter host cells by the well-established vectorial translocation mechanism that functions for YopE, YopH, and YpkA and thereby be sequestered from access to antibody. Indeed, tests with chimeric proteins consisting of N-terminal portions of YopM fused to the adenylate cyclase domain of the *Bordetella pertussis* hemolysin-adenylate cyclase have indicated that some of the chimeric YopM is translocated into cells. However, the fraction that was vectorially targeted in that study was relatively low (15). This left the significance of intracellularly targeted YopM unresolved and did not rule out an extracellular site of YopM function.

It is possible that YopM's virulence mechanism is not neutralizable by antibody, even though YopM might have an extracellular function. For example, if YopM has an environmentally modulated conformation, its putative active site might not be accessible to antibody because it is sequestered within the protein. We were intrigued by the finding that YopM could partially restore virulence to the YopM<sup>-</sup> *Y. pestis* strain without exacerbating a *Listeria* infection. This suggests that YopM in fact can have a virulence-related effect from an extracellular location but that the effect is *Yersinia*-specific - perhaps because YopM acts in concert with another *Yersinia* component. If added YopM needs to interact with yersiniae to exert its effect, the failure of exogenous YopM to restore complete virulence to the YopM<sup>-</sup> *Y. pestis* could have been due to the inability of the added YopM to reach foci of infection in sufficient concentration. Moreover, lethality is a relatively stringent readout of pathogenicity; we believe that the enhanced virulence of the YopM<sup>-</sup> *Y. pestis* in mice treated with YopM is significant and merits further study.

Our previous (3) and recent (detailed below) studies of thrombin-binding by YopM are consistent with a major virulence role of YopM other than thrombin-sequestration. This raises the issue of possible other targets for YopM, including intracellular ones. In the experiments of Aim 3, we examined the fates of exogenously added YopM and of YopM secreted by yersiniae to clarify the functions of this important *Yersinia* virulence protein.

## Roles of CD4<sup>+</sup> and CD8<sup>+</sup> T cells in defense against a primary infection with *Y. pestis*

**Rationale** To provide a more complete picture of the relevant defenses against *Y. pestis*, we conducted two pilot studies that compared the importance of CD8<sup>+</sup> and CD4<sup>+</sup> T cells in the defense against plague by naïve mice. If CD8<sup>+</sup> T cells provide an important host response to plague, then it might be possible in the future to devise an immunization protocol that would stimulate the response by these T cells, and this type of vaccination could be used to strengthen vaccines based on eliciting a purely humoral (antibody) response (due to CD4<sup>+</sup> T cells).

Our approach was to determine the virulence of *Y. pestis* in knockout mice unable to express CD4<sup>+</sup> or CD8<sup>+</sup> cells, C57BL/6-Cd4<sup>-</sup> and C57BL/6-Cd8a<sup>-</sup>, respectively (Jackson Laboratories). Because these CD4 and CD8 mutations were in a genetic background we had not previously tested for susceptibility to *Y. pestis*, we first determined rough LD<sub>50</sub> values for our parent *Y. pestis* KIM5 in the parent C57BL/6 mice. Groups of 3 female, 6-week-old mice were challenged retroorbitally intravenously (IV) with serial decimal doses of yersiniae as we previously described (16), and day of death was monitored for at least 14 d. The LD<sub>50</sub> for the parent *Y. pestis* KIM5 was < 10<sup>1</sup> (Table 4). This high susceptibility meant that we could not use the parent *Y. pestis* for these experiments, because the mutant mice would be expected to be more susceptible to *Y. pestis*, not less susceptible, and this would not be measurable (i.e., there is no inoculum range significantly less than 10<sup>1</sup> bacteria). Accordingly, we determined whether we had a mutant *Y. pestis* KIM5 strain that would be less virulent than *Y. pestis* KIM5 in C57BL/6 mice (Table 4).

**Table 4. LD<sub>50</sub> of *Y. pestis* KIM5 mutants for C57BL/6 mice**

Strain	Characteristics	LD <sub>50</sub>	Source or Reference
<i>Y. pestis</i> KIM5	parent Pgm <sup>-</sup> strain	< 10 <sup>1</sup>	R. R. Brubaker
<i>Y. pestis</i> KIM5-3001.1	psaA3::m-Tn3Cm (pH 6 Ag <sup>-</sup> )	< 10 <sup>2</sup>	71
<i>Y. pestis</i> KIM5-3001.17	yscP1 (Deletion of aa 246 - 333 of YscP)	< 10 <sup>1</sup>	P. Payne, lab stock
<i>Y. pestis</i> KIM53233 pHAElIII	YopM <sup>+</sup> due to overexpression of YopM in YopM <sup>-</sup> mutant	5 x 10 <sup>3</sup>	3
<i>Y. pestis</i> KIM5-3301 pV	LcrV <sup>+</sup> due to overexpression of LcrV; also YopJ <sup>-</sup>	3 x 10 <sup>1</sup>	72
<i>Y. pestis</i> KIM5-3131	YopK <sup>-</sup> YopL <sup>-</sup>	4 x 10 <sup>4</sup>	73

Of the mutants tested, *Y. pestis* KIM5-3131 (YopK<sup>-</sup>YopL<sup>-</sup>) presented the characteristics we needed: it still was virulent, but its virulence was decreased by several orders of magnitude compared to the parent *Y. pestis* KIM5 (Table 4), so that increased virulence in mutant mice could be measured. Importantly, the YopK<sup>-</sup>YopL<sup>-</sup> mutation is thought to

act by enlarging the "pore" through which Yops are conducted into host cells (17), rather than by inactivating any one virulence property. Accordingly, we hoped that the mutation would have more of a quantitative effect on the host response to the YopK<sup>-</sup>YopL<sup>-</sup> *Y. pestis* instead of qualitatively affecting the host response (e.g., by restoring a cytokine response that is inhibited by the wildtype *yopKL* gene in the parent *Y. pestis*).

We made two tests for the roles of CD4<sup>+</sup> and CD8<sup>+</sup> T cells in the defense of naïve mice against *Y. pestis*: comparison of the LD<sub>50</sub> of *Y. pestis* KIM5 to that of the YopK<sup>-</sup>YopL<sup>-</sup> *Y. pestis* in CD4<sup>-</sup> and CD8<sup>-</sup> mice and determination of the infection timecourses of the two *Y. pestis* strains in mice challenged with a fixed dose of yersiniae. In these tests, we used 3 mice per dosage group or infection time point. The LD<sub>50</sub> test was done as previously (i.e., female mice ca. 6 weeks old challenged IV retroorbitally and monitored at least 14 d).

**Table 5. LD<sub>50</sub> of YopK<sup>-</sup>YopL<sup>-</sup> *Y. pestis* in CD4<sup>-</sup> and CD8<sup>-</sup> mice.**

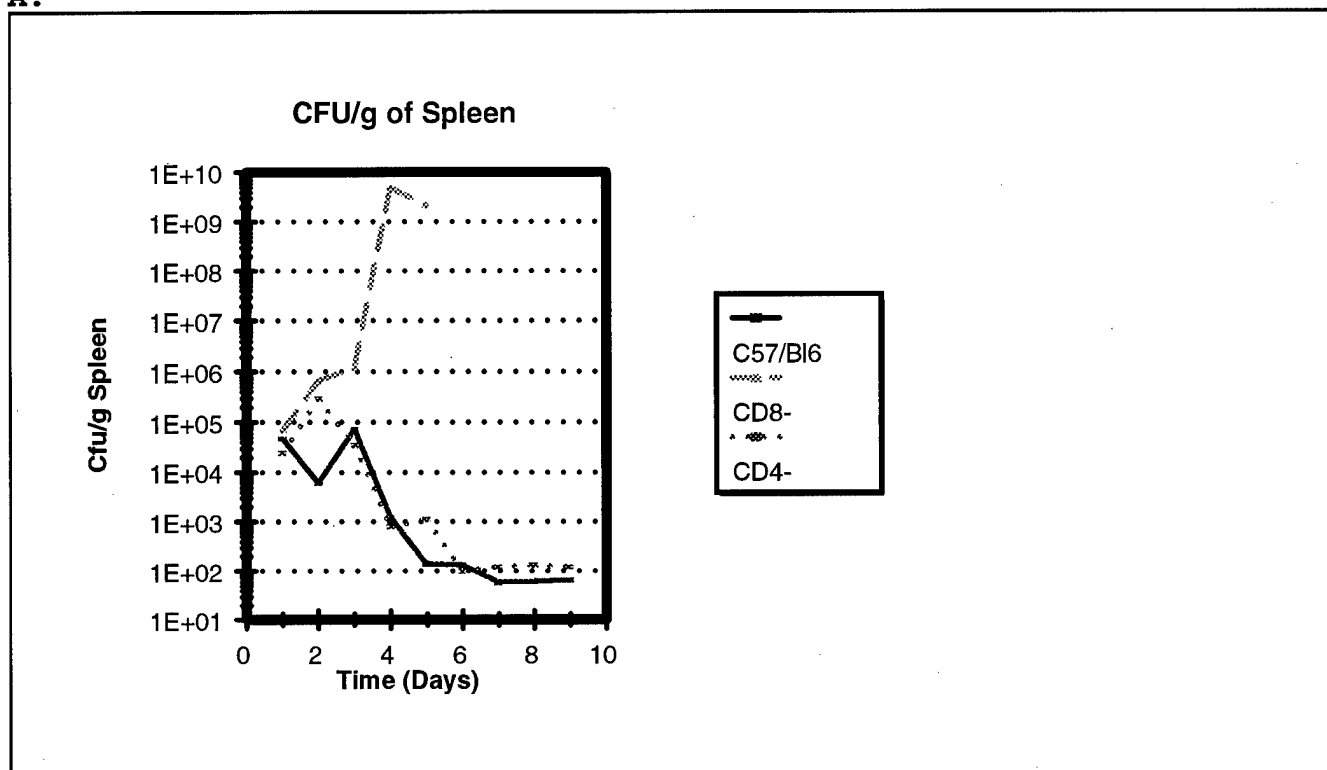
Mouse Strain	LD <sub>50</sub> of <i>Y. pestis</i> KIM5-3131
C57BL/6-CD4-<TmlMak>	1 x 10 <sup>3</sup>
C57BL/6-Cd8a<tmlMak>	2 x 10 <sup>2</sup>

The absence of CD4<sup>+</sup> T cells caused ca. a ten-fold increased virulence of *Y. pestis* KIM5-3131, whereas the absence of CD8<sup>+</sup> T cells resulted in ca. a 100-fold increase (Table 5).

To see if these differences in LD<sub>50</sub> values were meaningful, we infected mice with a dose of 4 x 10<sup>3</sup> *Y. pestis* KIM5-3131. This dose was greater than the LD<sub>50</sub> dose for the CD8<sup>-</sup> mice but less than that for the parent C57BL/6 mice. Three mice were euthanatized daily for 9 days, and CFU were determined for each mouse for spleen, liver, and lung (Fig. 1).

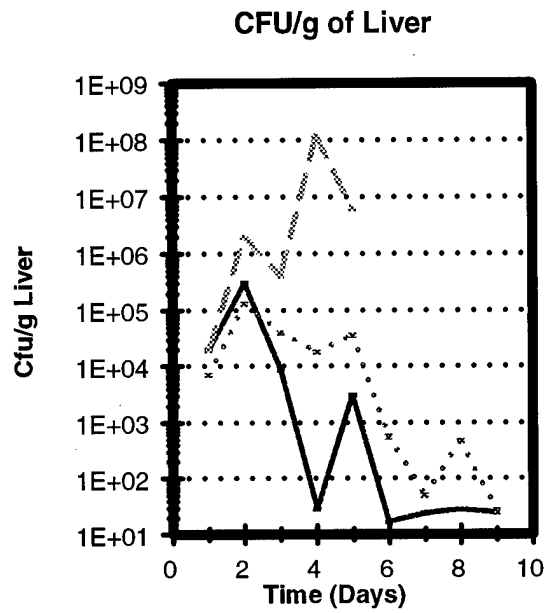
Figure 1. Infection timecourse for *Y. pestis* KIM5-3131 in C57BL/6, C57BL/6-CD4<sup>-</sup>Tm1Mak, and C57BL/6-CD8a<sup>-</sup>Tm1Mak mice. CFU were determined for spleens (panel A), liver (Panel B), and lung (Panel C).

A.

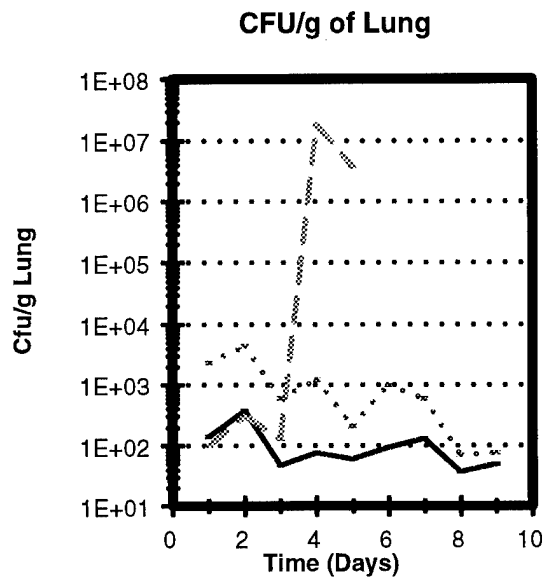


The parent mice cleared the yersiniae from spleen and liver in ca. 4 days, and the infection never became significant in the lung. In contrast, the CD8<sup>-</sup> mice were unable to control the infection, and the mice not euthanatized before day 5 were overwhelmed by plague and died. The CD4<sup>-</sup> mice behaved more like the parent mice, as though the LD<sub>50</sub> dose for *Y. pestis* KIM5-3131 in these mice actually was below the  $4 \times 10^3$  challenge dose.

B.



C.



## Discussion of findings on relative roles of CD4<sup>+</sup> and CD8<sup>+</sup> T cells in defense of naïve mice against plague

Both the virulence test and the infection timecourse gave the surprising finding that CD8<sup>+</sup> T cells, more than CD4<sup>+</sup> T cells, are an important component of the innate defenses against *Y. pestis* in C57BL/6 mice. It is possible that these cells make their contribution through production of cytokines such as IFN $\gamma$  early in infection and thus contribute to early macrophage activation, which is believed to be important for clearance of intracellular pathogens such as *Y. pestis*. Alternatively, perhaps CD8<sup>+</sup> T cells are acting as cytotoxic cells. In this case, the yersiniae that elicit the cytotoxic response presumably are intracellular, with antigens being presented on the surface of infected cells via MHC class I molecules. In either case, there are rapidly activatable CD8<sup>+</sup> T cells that presumably home to foci of infection by *Y. pestis* and are functional within the first 3 days of infection. We do not know if this is unique to C57BL/6 mice. An implication of these findings is that *Y. pestis* may have an intracellular niche during systemic infection (our model is for systemic plague). To have a complete picture of host-parasite interactions during plague, it will be important to determine the nature of that niche and the virulence properties that enable *Y. pestis* to reside there. Further, it may prove possible to develop vaccines aimed at enhancing the human CD8<sup>+</sup> response that targets intracellular yersiniae. We feel that further study of the immune response to *Y. pestis* will provide both valuable insight and potential benefit to persons exposed to plague.

## Aim 2 Determine if thrombin-binding is necessary for YopM function in vivo

TO 1 and TO 2. Identify thrombin-binding sites on YopM and eliminate thrombin-binding to YopM by site-directed mutagenesis of yopM

Introduction. A model has been proposed in which YopM significantly contributes to the virulence of *Y. pestis* by acting as an anti-inflammatory agent (18). YopM might function by sequestering thrombin. The resulting decreased clotting and inflammation would promote bacterial spreading and cripple the body's ability to deliver bactericidal cells to the focus of infection. To assess the significance of YopM's thrombin-binding in virulence, we created and tested the virulence of *Y. pestis* strains expressing mutant YopM molecules.

YopM belongs to a family of proteins that contain a leucine-rich repeat (LRR) motif (19). In porcine ribonuclease inhibitor, the prototype LRR protein for which X ray data are available, these tandem repeats create an extended "horseshoe"-like structure of parallel  $\beta$  strands connected by  $\alpha$ -helices (20,21). YopM was predicted by Kobe and Deisenhoffer (19) to have 12 tandem repeats, however we saw that a potential 13th repeat at the beginning of the stretch of repeats could be arranged. YopM

also has significant homology in its predicted sequence with the  $\alpha$ -chain of GPIb human platelet surface receptor. GPIb $\alpha$  also is an LRR family member, and its LRR structure was the basis of the homology to YopM. However, it is the only other LRR family member known to bind thrombin. The only commonality that emerges among the more than 40 LRR proteins is that they interact with other proteins, many functioning at the cell surface.

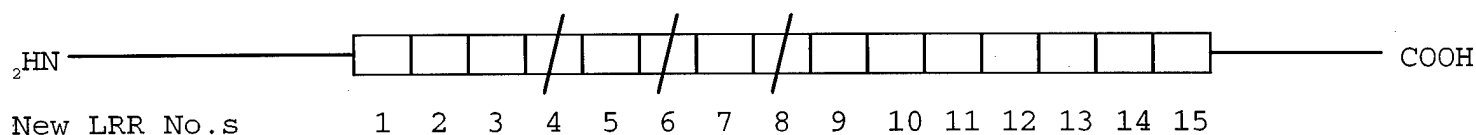
$\alpha$ -Thrombin is a serine protease with many structural similarities to trypsin but with a much greater specificity (22-24). Its active site is in a deep pocket partially occluded by two protruding loops that limit access of potential substrates. Moreover, thrombin's activity on protein substrates (as opposed to small-molecule synthetic substrates) requires binding of the substrate at one or more regions distinct from the catalytic site named "exosites". The catalytic pocket is flanked on the "west" and "east" by an apolar binding site and the anion-binding exosite I (abeI, also called the fibrinogen recognition exosite), respectively, and on the "north" by anion binding exosite II (abeII, the heparin binding site on thrombin). Abe I and II represent positively charged patches on the surface of thrombin (24,25). Substrates (fibrinogen, thrombin receptor, coagulation factor VIII), most exogenous inhibitors (the leech anticoagulant hirudin, the sulfated dodecapeptide representing hirudin's C-terminal tail called hirugen, an oligonucleotide aptamer), and activity modulators (thrombomodulin) bind to abeI by means of linear peptide sequences having clusters of negatively charged residues interspersed with hydrophobic residues that insert into the hydrophobic crevices of abeI. The endogenous thrombin inhibitor heparin cofactor II, following its interaction with heparin, also interacts with abeI. There is no strict consensus sequence for the abeI-binding regions of these molecules (23). Models for how they bind to abeI are based on information from the crystal structures of  $\alpha$ -thrombin bound to hirudin, to hirugen, and to peptides derived from the tethered-ligand thrombin receptor (26-29). Hirudin, a 65-residue peptide, has an N-terminal disulfide-knotted head that associates with the apolar site on thrombin and a C-terminal anionic tail. The tail binds in an extended conformation to abeI (27,30).

Revised sequence of YopM. Frederick Blattner's group at the University of Wisconsin-Madison Laboratory of Genetics completed the sequencing of the *Y. pestis* KIM LCR plasmid, and this sequence showed that YopM actually has 15 LRRs instead of 13. In our original sequencing of YopM (18), we had been confounded by regions of exactly duplicated nucleotide sequence, with the result that two LRRs had been omitted. We had begun to check the *yopM* sequence because of findings from mutant *yopMs* (described below) and continued that effort after the funds from the Collaborative Agreement had ended. We confirmed the results of the Blattner group by resequencing the entire *yopM* of *Y. pestis* KIM5 present on the YopM-overexpressing plasmid pBS10 that we had used for the purification of YopM for protection studies. We

also confirmed the sequence of the region specifying LRRs 3-10 (new LRR numbering) for the *yopM* gene on pBS15/15 used for mutagenesis and on *yopM* amplified from our current stock of *Y. pestis* KIM5. These all agreed with the Blattner group sequence. YopM, accordingly, is a 46,203 Da protein with predicted pI of 4.36.

The diagram below illustrates YopM's LRR structure.

**Figure 2. Diagram of the LRR structure of YopM. The boundaries of two highly similar regions are demarcated by /.**



The revised YopM nucleotide and predicted amino acid sequences are given on the next page.



atgttcataaatccaagaaatgtatctaatacttttttgcagaaccattacgtcattct  
 M F I N P R N V S N T F L Q E P L R H S  
 tctaatttaactgagatgccggttgaggcagaaaatgttaaatactagactgaatattat  
 S N L T E M P V E A E N V K S K T E Y Y  
 aatgcatggctcggaatgggaacgaaatgcccctccggggaatggtgaacagagggaaatg  
 N A W S E W E R N A P P G N G E Q R E M  
 gcggtttcaaggttacgagattgcctggaccgacaagcccattgagctagaactaaataat  
 A V S R L R D C L D R Q A H E L E L N N  
 ctggggctgagttctttgccggaattacctccgcatttagagagtttagtggcgctcatgt  
 L G L S S L P E L P P H L E S L V A S C  
 aattctcttacagaattaccggaattaccgcagagcctgaaatcacttctagttgataat  
 N S L T E L P E L P Q S L K S L L V D N  
 aacaatctgaaggcattatccgatttaccacctttactggaatatttaggtgtctctaata  
 N N L K A L S D L P P L L E Y L G V S N  
 aatcagctggaaaaatggcagagttgcaaaactcgctccttcttgaaaattattgatgtt  
 N Q L E K L P E L Q N S S F L K I I D V  
 gataacaattcactgaaaaaactacctgatttacctccttactggagtttattgctgct  
 D N N S L K K L P D L P P S L E F I A A  
 ggtaataatcagctggaagaattgccagagttgcaaaacttgcccttcttgactgcgatt  
 G N N Q L E E L P E L Q N L P F L T A I  
 tatgctgataacaattcactgaaaaaactacctgatttacctccttactggaatctatt  
 Y A D N N S L K K L P D L P L S L E S I  
 gttgctggtaataatattctggaagaattgccagagttgcaaaacttgcccttcttgact  
 V A G N N I L E E L P E L Q N L P F L T  
 acgatttatgctgataacaatttactgaaaacattacccgatttacccttccctggaa  
 T I Y A D N N L L K T L P D L P P S L E  
 gcacttaatgtcagagataattatttaactgatctgccagaattaccgcagagtttaacc  
 A L N V R D N Y L T D L P E L P Q S L T  
 ttcttagatgtttctgaaaatatttttctggattatcggaattgccacaaacttgat  
 F L D V S E N I F S G L S E L P P N L Y  
 tatctcaatgcatccagcaatgaaataagatccttatgagatttacccttactggaa  
 Y L N A S S N E I R S L C D L P P S L E  
 gaacttaatgtcagtaataataagttgatcgaaactgccagcggttacctccacgcttagaa  
 E L N V S N N K L I E L P A L P P R L E  
 cgtttaatcgcttcatttaatcatcttgctgaagtacctgaattgccgcaaaactgaaa  
 R L I A S F N H L A E V P E L P Q N L K  
 cagctccacgtagagtacaacctctgagagagtttcccgatatacctgagtcagtgga  
 Q L H V E Y N P L R E F P D I P E S V E  
 gatcttcggatgaactctgaacgtgtagttgatccatatgaatttgctcatgagactaca  
 D L R M N S E R V V D P Y E F A H E T T  
 gacaaacttgaagatgatgtatttgagtag  
 D K L E D D V F E -

The arrangement of YopM into LRRs is given below.

<u>YopM</u>		<u>New #</u>	<u>Old</u>
1	MFINPRNVSNTFLQEPLRHSSNLTEMPVEAENVKSK	36	
37	TEYYNAWSEWERNAPPGNGEQREMAVSRLRDCLDR	71	
72	QAHELELNGLSSLPPELPP	91	LRR 1 1
92	HLESLVASCNSLTPELPQ	111	LRR 2 2
112	SLKSLLDVNNNLKALSDLPP	131	LRR 3 3
132	LLEYLGVSNNQLEKLPELQNSS	153	LRR 4 4/4'
154	FLKIIDVDNNSLKKLPDLPP	173	LRR 5 5'
174	SLEFIAAGNNQLEELPELQNL	195	LRR 6 6'/4
196	FLTAIYADNNSLKKLPDLPL	215	LRR 7 5
216	SLESIVAGNNILEELPELQNL	237	LRR 8 6
238	FLTTIYADNNLLKTLPELPP	257	LRR 9 7
258	SLEALNVRDNYLTDLPELPQ	277	LRR 10 8
278	SLTFLDVSENIFSGLSELPP	297	LRR 11 9
298	NLYYLNASSNEIRSLCDLPP	317	LRR 12 10
318	SLEELNVSNNKLIELPALPP	337	LRR 13 11
338	RLERLIASFNLAEVPELPQ	357	LRR 14 12
358	NLKQLHVEYNPLREFPDIP	377	LRR 15 13
378	SVEDLRMNSERVVDPYEFAHETTDKLEDDVFE	409	

Construction of mutant yopM genes expressing YopM proteins with defective thrombin-binding.

Construction of yopMS and yopMR. To test the importance for thrombin-binding of the C-terminal 16 YopM residues, containing 7 acidic (D,E) and three basic (R,K) amino acids, we made two constructs: YopMS was missing these and had two hydrophobic residues (A,V) added at the C-terminus, and YopMR replaced the C-terminal 15 residues with 14 irrelevant residues encoded by the pBR322 vector. The plasmid pBS-6 was cleaved with NdeI and religated. This plasmid carries the same insert as pBS7, and inserted into the same vector (3), but in the opposite orientation. It has 3 NdeI sites, one near the end of yopM and two within the vector. YopMR and S resulted from cleavages at the site within yopM and at the proximal and distal other two sites, respectively.

Characterization of YopMS and YopMR. Plasmids pBS6-2 and pBS6-3 carrying yopMS and yopMR, respectively, were transformed into a YopM strain of *Y. pestis* KIM that was lacking the pPCP1 plasmid that encodes the Pla protease that degrades Yops. The resulting strains were grown as 3.2-L cultures, induced for Yops expression and the YopM proteins isolated as previously described (3,16). YopMS and R were strongly expressed and secreted. Because YopM is acidic throughout its length, these truncated YopMs had isoelectric points similar to YopM, and these proteins purified similarly to YopM upon anion exchange chromatography.

## Results and discussion - YopMS and YopMR

Both YopMS and YopMR bound to thrombin and could be crosslinked (as in Refs. 3,33) to form the ca. 75 kDa YopM-thrombin complex. YopMR may have interacted slightly less efficiently than did YopM, while YopMS consistently appeared to bind thrombin more tightly than does YopM, giving more crosslinked product. The binding of both YopMS and YopMR to thrombin was at thrombin's abel, because it was outcompeted by hirudin and the aptamer R15 (33). The interaction was specific, because it was not outcompeted by the scrambled aptamer S15 (33). These data showed that the C-terminal-most amino acids of YopM are not necessary for thrombin-binding; if anything, they make the interaction with thrombin less efficient. Together, these data indicated that YopMR and YopMS interacted essentially normally with thrombin.

## Construction of yopM genes expressing internally deleted YopMs.

General strategy. We wanted to test whether various LRRs of YopM are responsible for thrombin-binding, but wanted to avoid grossly deranging the protein's structure. Although we do not know YopM's 3° structure, we used its LRR architecture as a basis for a rough model for how YopM might appear if it followed the pattern of porcine RNase inhibitor, and subsequently, Andrey Kajava of the Swiss Institute for Experimental Cancer Research constructed a detailed molecular model which agreed in essence with our rough model. The resulting picture revealed the possibility of remarkable distribution of charge within YopM: residue 17 of each 20- or 22-residue LRR is negatively charged and predicted to be exposed on the outside of the protein. These residues would make one face of the molecule very negatively charged. The opposite face also would be charged around most of the protein, due to residues # 11, 13, and 14 of each LRR; however, in various LRRs these may differ. Because the protein probably is highly structured, we felt it important to preserve its LRR arrangement and not delete part of an LRR, which might make an unaccommodated kink in the molecule. Moreover, because some LRRs alternated in the presence of + and - charge in the connecting strands, we were reluctant to disrupt that pattern. Accordingly, we chose to delete pairs of LRRs.

To make the deletions, we followed the strategy of Wren et al. (74) and designed primers in opposite orientations at a gap that defined the deletion to be made in *yopM*. The 5' end of each primer contained the *yopM* sequence altered by 1 or 2 bases so as to create a restriction site for a blunt-end-creating restriction enzyme without changing the amino acids normally encoded by that part of *yopM*. A PCR reaction would then initiate at both primers, extending in opposite directions and running around the entire plasmid template. The PCR products were digested with the restriction enzyme for which sites were present in the primers and religated. This created plasmids containing the desired deletion within *yopM*. The plasmids were transformed into *E. coli* XL1 Blue with selection for the ampicillin-resistance on the pBR322-derived vector (100 µg/ml ampicillin) and

were reisolated from selected colonies for confirmation of their restriction maps.

# Details of the constructions.

Construction of pBS15/15. We modified pBS15 (3), which includes ca. 780 bp of DNA upstream of *yopM*, for our deletion work. Because the PCR reactions had to extend through the entire plasmid, we first made the plasmid smaller. We deleted most of this upstream sequence by cleaving with *MscI* and *Bst* 1107I and religating. This created pBS15/15, 3699 bp in size. It also converted the plasmid from one that does not overexpress *YopM* to one that does by removing the upstream sequence that down-modulates *yopM* expression (3).

**Table 6. Primers for the deletion of LRRs in *YopM*.**

Primer	Sequence and Restriction Site
<u>LRRs 1-2; Obtained <math>\Delta</math>LRRs 1-7</u>	
	<i>Afl</i> III
P1-2 down	5'AGG TAC <u>CTT AAG</u> GCT TCG GTC CAG GCA ATC TCG TAA CCT TGA 3'
P1-2 up	5'GTAC AGC <u>CTT AAG</u> TCA CTT CTA GTT GAT AAT AAC AAT CTG AAG GCA 3'
<u>LRRs 4-5; Obtained: <math>\Delta</math>LRR4-5</u>	
	<i>Sma</i> I
P4-5 down	5'TACG <u>CCC GGG</u> TAA ATC GGA TAA TGC CTT CAG ATT 3'
	<i>Stu</i> I
P4-5 up	5'TACG <u>AGG CCT</u> TCA CTG GAA TCT ATT GTT GCT GGT 3'
<u>LRRs 6-7; Obtained: <math>\Delta</math>LRR6-7, <math>\Delta</math>LRR4-7, <math>\Delta</math>LRR2-7, and <math>\Delta</math>LRR7</u>	
	<i>Sma</i> I
P6-7 down	5'TACG <u>CCC GGG</u> TAA ATC AGG TAG TTT TTT CAG TGA ATT 3'
	<i>Ecl</i> 136II
P6-7 up	5'TACG <u>GAG CTC</u> TCC CTG GAA GCA CTT AAT GTC AGA 3'
<u>LRRs 7-8; Obtained: <math>\Delta</math>LRR7-8 and <math>\Delta</math>LRR 5-8</u>	
	<i>Sma</i> I
P7-8 down	5'GATC <u>CCC GGG</u> AG GTT TTG CAA CTC TGG CAA 3'
	<i>Eco</i> RV
P7-8 up	5'GATC <u>GAT ATCC</u> TTA ACC TTC TTA GAT GTT TCT GAA AAT ATT 3'

LRRs 4-7; Obtained: ΔLRR 4-7

P4-5 down

P6-7 up

LRRs 7-13; Obtained: ΔLRR 7-13

P7-8 down

*EcoRV*

P12-13 up 5'GATC GAT ATC GG TGG AA GAT CTT CGG ATG AAC TCT 3'

NH<sub>2</sub>(aa19) - LRR4; Obtained NH<sub>2</sub>-5

*SmaI*

PNH<sub>2</sub> down 5'TGC TAG CCC GGG TTC TTG CAA AAA AGT ATT AGA TAC ATT TCT 3'

P4-5 up

NH<sub>2</sub>(aa19) - LRR6; Obtained NH<sub>2</sub>-ca.6, NH<sub>2</sub>-8, and NH<sub>2</sub>-ca.9

PNH<sub>2</sub> down

P6-7 up

Construction of specific deletions. The primer pairs used for the deletions are given in Table 6. Because of the highly repetitive nature of *yopM* (18), it was difficult to identify primers that would not prime at multiple sites. Some of our primers produced a family of deletions, and some produced unexpected deletions (Table 6). Both of these events expanded the array of products for analysis. Table 7 lists the constructs obtained from the deletion mutagenesis. The actual boundaries of all deletions are not known, because not all constructs have been sequenced throughout the LRR region and because the PCR reactions used to generate the constructs could give rise to more than one product. The designation used for most of the mutant YopMs in Table 7 is based on restriction mapping of the constructs encoding them, on limited sequence information, and on the assumption that YopM had only 13 LRRs. The genes encoding YopMs that were used in detailed studies were sequenced, and their YopM designations have a parentheses giving the actual deleted LRRs according to the new numbering of LRRs.

The constructs were transformed into the YopM<sup>-</sup> Pla<sup>-</sup> *Y. pestis* KIM8-3233 and grown as we did for the YopMS and YopMR constructs, to express the mutant YopM proteins. All constructs except the series deleting after residue 18 (denoted NH<sub>2</sub>-x) strongly produced their internally deleted proteins. The NH<sub>2</sub>-9 construct did not produce a recognizable YopM protein. The NH<sub>2</sub>-ca.6, NH<sub>2</sub>-ca.8, and NH<sub>2</sub>-ca.5 constructs do make their protein but not strongly.

Table 7. Mutant YopMs obtained and their strength of expression in *Y. pestis* KIM8-3233.

<u>YopM</u>	<u>Expression</u>	<u>YopM</u>	<u>Expression</u>
YopM	++	YopM $\Delta$ LRR4-5 (4-7)	++
YopMS	++	YopM $\Delta$ LRR4-7 (4-9)	++
YopM $\Delta$ LRRNH <sub>2</sub> -5	+	YopM $\Delta$ LRR6-7 (6-9)	++
YopM $\Delta$ LRRNH <sub>2</sub> -6	+	YopM $\Delta$ LRR7 (8-9)	++
YopM $\Delta$ LRRNH <sub>2</sub> -8	+	YopM $\Delta$ LRR5-8	++
YopM $\Delta$ LRRNH <sub>2</sub> -9	-	YopM $\Delta$ LRR7-8 (7-10)	++
YopM $\Delta$ LRR1-7	++	YopM $\Delta$ LRR7-13	++
YopM $\Delta$ LRR2-7	++		

Five mutant YopMs were characterized in detail. Their actual sequences are given below.

" $\Delta$ LRR4-5" (4-7)

1	MFINPRNVSNTFLQEPLRHSSNLTEMPVEAENVKSK	36	
37	TEYYNAWSEWERNAPPGNGEQREMAVSRLRDCLDR	71	
72	QAHELELNNLGLSSLPELPP	91	LRR 1
92	HLESLVASCNSLTPELPQ	111	LRR 2
112	SLKSLLDVNNNLKALSDLPP	131	LRR 3
//		//	
216	SLESIVAGNNILEELPELQNLPP	237	LRR 8
238	FLTTIYADNNLLKTLPLDLP	257	LRR 9
258	SLEALNVRDNYLTDLPELPQ	277	LRR 10
278	SLTFLDVSENIFFSGLSELPP	297	LRR 11
298	NLYYLNASSNEIRSLCDLPP	317	LRR 12
318	SLEELNVSNNKLIELPALPP	337	LRR 13
338	RLERLIASFNHLAEVPELPQ	357	LRR 14
358	NLKQLHVEYNPLREFPDIP	377	LRR 15
378	SVEDLRMNSERVDPYEFAHETTDKLEDDVFE	409	

"ΔLRR4-7" (4-9)

1	MFINPRNVSNFTLQEPLRHSSNLTEMPVEAENVKSK	36	
37	TEYYNAWSEWERNAPPGNGEQREMAVSRLRDCLDR	71	
72	QAHELELNNLGLSSLPELPP	91	LRR 1
92	HLESLVASCNSLTPELPPQ	111	LRR 2
112	SLKSLLDVNNNLKALSDLPP	131	LRR 3
	//	//	
258	SLEALNVRDNYLTDLPELPPQ	277	LRR 10
278	SLTFLDVSENIFFGLSELPP	297	LRR 11
298	NLYYLNASSNEIRSLCDLPP	317	LRR 12
318	SLEELNVSNKKLIELPALPP	337	LRR 13
338	RLERLIASFNLAEVPELPPQ	357	LRR 14
358	NLKQLHVEYNPLREFPDIP	377	LRR 15
378	SVEDLRMNSERVVDPYEFAHETTDKLEDDVFE	409	

"ΔLRR6-7" (6-9)

1	MFINPRNVSNFTLQEPLRHSSNLTEMPVEAENVKSK	36	
37	TEYYNAWSEWERNAPPGNGEQREMAVSRLRDCLDR	71	
72	QAHELELNNLGLSSLPELPP	91	LRR 1
92	HLESLVASCNSLTPELPPQ	111	LRR 2
112	SLKSLLDVNNNLKALSDLPP	131	LRR 3
132	LLEYLGVSNNQLEKLPELQNSS	153	LRR 4
154	FLKIIDVDNNSLKKLPDLPP	173	LRR 5
	//	//	
258	SLEALNVRDNYLTDLPELPPQ	277	LRR 10
278	SLTFLDVSENIFFGLSELPP	297	LRR 11
298	NLYYLNASSNEIRSLCDLPP	317	LRR 12
318	SLEELNVSNKKLIELPALPP	337	LRR 13
338	RLERLIASFNLAEVPELPPQ	357	LRR 14
358	NLKQLHVEYNPLREFPDIP	377	LRR 15
378	SVEDLRMNSERVVDPYEFAHETTDKLEDDVFE	409	

"ΔLRR7" (8-9)

1	MFINPRNVSNTFLQEPLRHSSNLTEMPVEAENVKSK	36	
37	TEYYNAWSEWERNAPPGNGEQREMAVSRLRDCLDR	71	
72	QAHELELNNLGLSSLPELPP	91	LRR 1
92	HLESLVASCNSLTPELPPQ	111	LRR 2
112	SLKSLLDVNNNLKALSDLPP	131	LRR 3
132	LLEYLGVSNNQLEKLPQLNSS	153	LRR 4
154	FLKIIDVDNNSLKKLPDLPP	173	LRR 5
174	SLEFIAAGNNQLEELPELQNL	195	LRR 6
196	FLTAIYADNNSLKKLPDLPL	215	LRR 7
//		//	
258	SLEALNVRDNYLTDLPELPPQ	277	LRR 10
278	SLTFLDVSENIFSGLSLPP	297	LRR 11
298	NLYYLNASSNEIRSLCDLPP	317	LRR 12
318	SLEELNVSNNKLIELPALPP	337	LRR 13
338	RLERLIASFNHLEVPPELPPQ	357	LRR 14
358	NLKQLHVEYNPLREFPDIP	377	LRR 15
378	SVEDLRMNSERVVDPYEFAHETTDKLEDDVFE	409	

"ΔLRR7-8" (7-10)

1	MFINPRNVSNTFLQEPLRHSSNLTEMPVEAENVKSK	36	
37	TEYYNAWSEWERNAPPGNGEQREMAVSRLRDCLDR	71	
72	QAHELELNNLGLSSLPELPP	91	LRR 1
92	HLESLVASCNSLTPELPPQ	111	LRR 2
112	SLKSLLDVNNNLKALSDLPP	131	LRR 3
132	LLEYLGVSNNQLEKLPQLNSS	153	LRR 4
154	FLKIIDVDNNSLKKLPDLPP	173	LRR 5
174	SLEFIAAGNNQLEELPELQNL	195	LRR 6
//		//	
278	SLTFLDVSENIFSGLSLPP	297	LRR 11
298	NLYYLNASSNEIRSLCDLPP	317	LRR 12
318	SLEELNVSNNKLIELPALPP	337	LRR 13
338	RLERLIASFNHLEVPPELPPQ	357	LRR 14
358	NLKQLHVEYNPLREFPDIP	377	LRR 15
378	SVEDLRMNSERVVDPYEFAHETTDKLEDDVFE	409	

These five YopMs were grown in 1.6-L cultures to produce and purify their YopM in sufficient amounts for analysis of thrombin-binding and for experiments of Aim 3. The profiles of these purified YopMΔLRRs in SDS-PAGE resembled that for similarly loaded YopM, except for their size. This, plus their strong expression and normal secretion by *Y. pestis*, indicated that these YopMΔLRRs are not grossly deranged or targets for proteolysis (however, see below for YopMΔLRR4-7[4-9]).

Results and discussion - YopMΔLRR proteins

We tested the five purified mutant YopMs and YopMS for their ability to bind α-thrombin by three assays: crosslinking by



disuccinimyl suberate (DSS) (performed as in refs. 3, 33), ELISA (protocol given below), and inhibition of thrombin-induced platelet aggregation (protocol given below). The ELISA proved to be poorly discriminatory; Table 8 summarizes the findings from the other two assays.

**Table 8. Ability of mutant YopMs to interact with human  $\alpha$ -thrombin, assayed by ability to form a chemically crosslinked product and by the ability to inhibit thrombin-elicited aggregation of human platelets.**

YopM	Crosslinking	Aggregation Inhibition <sup>a</sup>
YopM	+	9.4 $\pm$ 2.0
YopMS	+++	2.6 $\pm$ 0.9
YopM $\Delta$ LRR4-5(4-7)	+	7.5 $\pm$ 0.0
YopM $\Delta$ LRR7(8-9)	+	11.0 $\pm$ 3.0
YopM $\Delta$ LRR4-7(4-9)	-	12.5 $\pm$ 3.1
YopM $\Delta$ LRR6-7(6-9)	$\pm$	12.5 $\pm$ 2.0
YopM $\Delta$ LRR7-8(7-10)	-	15.0 $\pm$ 0.0

a = nM of YopM or mutant YopM required to completely inhibit  $\alpha$ -thrombin-induced platelet aggregation.

YopM $\Delta$ 4-5(4-7) and YopM $\Delta$ 7(8-9), appeared to interact normally with thrombin, forming the 1:1 crosslinked product with thrombin (as well as the characteristic spectrum of higher molecular weight forms normally seen in these assays) and being cleaved near the C-terminus by thrombin (33). Interestingly, even though YopM $\Delta$ 4-7(4-9) did not bind thrombin so as to be trapped in a complex by DSS crosslinks, this YopM $\Delta$ LRR nonetheless was cleaved by thrombin. This indicates that thrombin can act as a protease and cleave YopM independently of a crosslinkable interaction. For the mutant YopM, the interaction likely juxtaposes the two proteins without bringing crosslinkable free amines near enough to be linked by DSS.

The data show that LRRs 4 through 7 of YopM are not necessary for the specific binding of thrombin at the fibrinogen-binding site, abeI. These data do not assign thrombin-binding to a particular LRR but indicate that deletions more toward the C-terminus have stronger effects than those nearer the N-terminus: deletion of 4 LRRs had a larger effect if they were LRRs 7-10 than if they were 4-7. Dr. Andrey Kajava of the Swiss Institute for Experimental Cancer Research is subjecting YopM and the mutant YopMs to molecular modeling. This will show what residues are free to interact with thrombin and may help explain why YopM $\Delta$ LRR4-5(4-7) and YopM $\Delta$ LRR7(8-9) can bind thrombin at abeI and be crosslinked, in contrast to YopM $\Delta$ LRR4-7(4-9).

We applied two other assays for the interaction of YopM and thrombin to have better quantitation (the ELISA) and to have a measure of how the mutations affected YopM's ability to nullify thrombin function. It was conceivable that a deletion might remove YopM

residues that are involved in chemical crosslinking but have no effect on YopM's ability to inhibit thrombin function or vice versa.

### **Platelet Aggregation Assay**

Platelet-rich plasma (PRP) was isolated from 100 ml of freshly-drawn, citrated human blood by centrifugation at 200 x g for 10 min at room temperature in a Beckman TJ-6 tabletop centrifuge. The PRP layer was recovered from the remaining sample with a plastic pasteur pipet and transferred to a 50 ml, polypropylene conical centrifuge tube and held at room temperature (RT). The remaining blood sample was recentrifuged at 850 x g for 15 min at RT, and the platelet-poor plasma (PPP) fraction was removed to a separate 50 ml conical tube, again with a plastic pipet. The PPP was used to adjust the platelet concentration in the PRP fraction to  $\sim 3 \times 10^5$  cells/ml. Four hundred and fifty  $\mu$ l of the adjusted sample was added to a Chronolog cuvette containing a stirbar, and the cuvette was placed into the sample chamber of a Chronolog Model 340 Dual Chamber Aggregometer (Chronolog Corp., Havertown, PA) that had been prewarmed to 37°C. The sample was warmed in the chamber for one min before the addition of YopM or thrombin. Following this incubation period, purified YopM or YopM mutant proteins were added at various concentrations (2.5 - 15 nM) to the sample and allowed to incubate with the platelets for an additional minute. Following the incubation period a predetermined amount of human  $\alpha$ -thrombin (0.18-0.36 U, Haematologic Technologies Inc., Essex Jct., VT) was added to the sample and an increase in light transmission through the sample was detected by the aggregometer if thrombin-induced platelet aggregation had occurred. However, if YopM or the mutant proteins inhibited aggregation, the amount of light transmission through the sample increased only slightly or did not change.

### **Results and discussion - platelet aggregation assay**

In this assay, greater amounts of protein that have to be added to inhibit aggregation correspond to less efficient interactions of that protein with thrombin. Table 8 shows that only the mutation in YopMS had a significant effect on platelet aggregation, and this effect correlated with the greater amount of crosslinked product detected in SDS-PAGE profiles from the crosslinking assay. The data for the other mutants were not significantly different (at  $p=.05$ ) from those for YopM. Accordingly, these YopM proteins might still bind thrombin approximately as well as does YopM but may (e.g., YopM $\Delta$ LRR7[8-9]) or may not (e.g., YopM $\Delta$ LRR4-7[4-9]) have lysine residues on the apposing molecules, that are appropriately spaced for crosslinking to take place. However, platelet aggregation is a finicky assay, requiring standardization each day for the amount of thrombin and YopM to use, because of differences in the activity of the platelet preparations. Hence, the scatter from the assay may be masking small but real differences in YopM's thrombin-neutralization activity. YopM $\Delta$ LRR7-8(7-10) may actually have been impaired in its ability to inhibit thrombin-elicited platelet aggregation.

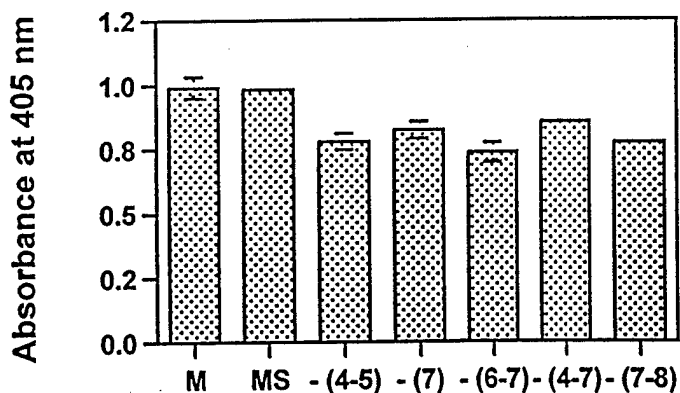
### Enzyme-linked immunosorbent assay (ELISA) to quantitate YopM-human $\alpha$ -thrombin binding.

Flat-bottom, 96-well, Nunc Maxisorp immunoplates (Fisher Scientific, Pittsburgh, PA) were coated with 100  $\mu$ l of YopM or YopM mutants (100  $\mu$ g/ml in PBS) at RT for 2 h (or overnight at 4°C). The wells were blocked with bovine serum albumin (200  $\mu$ l of a 5% [vol/vol] solution in PBS per well, 4°C, overnight) and washed thrice, 3 min each time, with PBS containing 0.05% (vol/vol) Tween 20 (Fisher) and 0.02% (wt/vol) sodium azide (Sigma) (PBS-TA). 100  $\mu$ l of human  $\alpha$ -thrombin (200  $\mu$ g/ml in PBS with 0.1% PEG) were added to triplicate wells for 2 h at 37°C. One hundred  $\mu$ l of PBS-TA alone or thrombin alone were added to control wells. The plates were then washed and coated for 2 h at 37°C with rabbit anti-human thrombin antibody (IgG) (American Diagnostica, Inc., Greenwich, CT) diluted 1:250 in PBS-TA. The wells were washed again and 100  $\mu$ l of alkaline-phosphatase-labeled goat anti-rabbit IgG diluted 1:15,000 (Sigma) was added to each for 2 h at 37°C. After another washing step, 100  $\mu$ l of Sigma Fast<sup>TM</sup> substrate (p-nitrophenyl phosphate) was added to each well, the plates were incubated at 37°C for 15 min, and the reaction was stopped by the addition of 25  $\mu$ l of 3N NaOH to each well.  $A_{405}$  nm was measured using a Maxkinetic microplate reader (Molecular Devices Corp., Menlo Park, CA). Average absorbance values were determined for each dilution of each serum sample minus the background absorbance (thrombin-only control wells). The adjusted absorbance values for YopM or YopM mutants were then plotted.

### Results and discussion - thrombin-binding ELISA

This ELISA for YopM's ability to bind thrombin gave findings consistent with those from the platelet aggregation inhibition assay but had even less sensitivity: there was no difference detected between YopM and YopMS and little decrease in  $A_{405}$  for the other mutant YopMs (Fig. 3).

**Figure 3. Ability of YopM and mutant YopMs to bind thrombin as measured by ELISA.**



C68S and C100S YopM. We found that we could crosslink YopM and thrombin with the heterobifunctional crosslinker SMCC (succinimidyl 4-[N-maleimidomethyl]cyclohexane-1-carboxylate), which targets a free SH and an  $\epsilon$ -NH<sub>2</sub> group, but not with the homobifunctional BMH (bismaleimido-hexane), which targets only SH groups. Because thrombin's 8 -SH are all tied up in intramolecular disulfide bonds, this finding indicates that one of YopM's 3 C must provide the SH for crosslinking with SMCC. If we could find which C was involved, this would tell us a region on YopM that becomes closely apposed to thrombin when the two proteins form a complex and would direct us to the region of YopM involved in thrombin-binding. Dr. Andrey Kajava had formulated a molecular model for YopM (based on the 13-LRR assumption), and he extended this to include a prediction for how YopM could bind thrombin. This model had the globular thrombin sitting on top of a curved "throne" of the horseshoe-shaped YopM. Accordingly, thrombin's abel engaged residues on several LRRs, rather than a linear peptide as in previously characterized thrombin substrates. Depending on which side of the horseshoe thrombin sat, C68 or C100 of YopM could be close enough to be crosslinked to an  $\epsilon$ -NH<sub>2</sub> group on thrombin. We tested this model by making two mutant YopMs, each having one of these cysteines replaced by serine.

The construction was done as described above for the  $\Delta$ LRR YopMs. The primers used are given below.

#### **Primers for site-directed mutagenesis of *yopM*.**

##### Construction of C68S YopM.

C68up 5' ATT CGC TTA AGA GAT **AGC** CTG GAC CGA CAA GCC 3'  
S68

C68down 5' TAA TCT TAA GCG TGA AAC CGC CAT TTC CCT CTG 3'

##### Construction of C100S YopM.

C100up 5' AGT TTA GTC GCG AGC **AGT** AAT TCT CTT ACA GAA TTA 3'  
S100

C100down 5' **ACT** GCT CGC GAC TAA ACT CTC TAA ATG CGG AGG 3'  
S100

The underlined nucleotides are different from the native *yopM* sequence and made two types of changes after the PCR. The large-font, bolded codons encoded the serines in the C68S and C100S mutant YopMs. The small-font italicized bases encoded new restriction sites, where the changed bases did not alter the encoded amino acids for the changed codons. For C68S *yopM*, the new site was *Afl*III; for C100S *yopM*, it was *Nm*I.

The resulting constructs were characterized by restriction analysis and nucleotide sequencing and were electroporated into *Y. pestis* KIM8-3233 (YopM<sup>+</sup> Pla<sup>-</sup>). The strains were grown and their mutant YopMs purified as for the  $\Delta$ LRR YopMs. They were then tested for

their ability to crosslink to thrombin with DSS, SMCC, DPDPB (1,4-Di-[3'-(2'-pyridyldithio)-propionamido]butane, a homobifunctional crosslinker targeting SH and having a spacer arm of 19.9 Å as opposed to 16.1 Å for BMH), and BMH (all obtained from Pierce Biochemicals, Rockford, IL). Briefly, YopM and thrombin were added to PBS (pH 7.4) at a final concentration of 5 µM in the presence of 0.1% polyethylene glycol. The sample was mixed and allowed to incubate at room temperature for 20 min. At this point, crosslinker was added to a final concentration of 5 mM and the samples allowed to incubate for 40 min at RT. If the thrombin inhibitor Hirudin (0.072 µg/ml) was used to block the reaction, it was preincubated with thrombin for 15 min before the addition of YopM or mutant YopM to the mixture. The reaction was terminated by the addition of Tris-HCl to a final concentration of 0.1 mM, and an equal volume of 2X SDS-PAGE sample buffer was added to each sample. Proteins were separated by standard SDS-PAGE (12% [wt/vol] acrylamide) and analysed by immunoblot.

### Results and discussion -- C68S and C100S YopM

Both C68S and C100S YopM showed the same spectrum of crosslinking as did YopM: + for DSS and SMCC, and - for BMH and DPDPB. These tests threatened Dr. Kajava's model for YopM-thrombin binding.

### Tests for which protein provides the S that crosslinks with SMCC

We attempted several tests aimed at determining if possibly the SH for SMCC crosslinking in fact came from thrombin and not YopM, or, conversely, that a SH on YopM was essential for this reaction as we previously thought. These tests are briefly described below.

### **Blocking Thrombin or YopM with N-ethyl maleimide (NEM)**

Blocking of free -SH groups on human α-thrombin or YopM was done following the method of Riordan and Valee (34). Briefly 0.001 M NEM was added to 1 ml of 0.1 M PO<sub>4</sub> buffer (pH 7.0) at RT in a quartz cuvette. Enough protein was added to this solution to decrease the A<sub>305</sub> from ~ 0.620 by 0.1 to 0.5 absorbance units. The tripeptide glutathione was used as a control to determine NEM's ability to block -SH groups.

### Results:

1. 500 µg ( $1.7 \times 10^{-6}$  M) of glutathione decreased the A<sub>305</sub> from 0.629 to 0.032 in approx. 2 min.
2. 1800 µg ( $5 \times 10^{-8}$  M) of Sigma α-thrombin did not change A<sub>305</sub> of sample even after 2 h incubation.
3. 630 µg ( $1.8 \times 10^{-8}$  M) of α-thrombin given to us by John Fenton (Wadsworth Center for Laboratories and Research, Albany, NY) - no change after 2 h.
4. 1000 µg ( $2.4 \times 10^{-8}$  M) YopM - no change after 2 h
5. 3000 µg BSA (fraction V) - 0.851 to 0.781 within 2 h

### Conclusions:

This method may not be sensitive enough to detect blockage of the

few -SH groups on YopM and  $\alpha$ -thrombin.

**Use of radiolabeled NEM ( $^3\text{H}$ -NEM) to detect blockage of -SH groups on thrombin**

~ 2  $\mu\text{Ci}$  of  $^3\text{H}$ -NEM (60 Ci/mmol; NEN Life Sciences Products, Boston, MA) were added to 830  $\mu\text{g}$  of Fenton's thrombin or an equimolar equivalent amount of glutathione in 1 ml 0.1 M  $\text{PO}_4$  buffer and allowed to incubate for 1 h or overnight (ON). 50  $\mu\text{l}$  of the sample was run over a Micro Bio-Spin Chromatography column (Bio-Rad Laboratories, Hercules, CA) equilibrated in 0.1 M  $\text{PO}_4$  buffer following the manufacturer's protocol. The column was necessary to remove unbound NEM. The cpm per sample were determined by scintillation counting.

Results:

DAY 1:

1. cpm of 50  $\mu\text{l}$  of NEM in  $\text{PO}_4$  buffer (not run over column): 7128.5
2. cpm of 50  $\mu\text{l}$  of NEM (run over column; = background cpm): 328.2
3. cpm of 50  $\mu\text{l}$  of NEM + thrombin (1 h incubation; over column): 302.4

DAY 2:

4. cpm of 50  $\mu\text{l}$  of NEM (at  $4^\circ\text{C}$ , ON; then run over column; = background): 116.3
5. cpm of 50  $\mu\text{l}$  of NEM + thrombin (ON at  $4^\circ\text{C}$ ; then run over column): 320.5
6. cpm of 50  $\mu\text{l}$  of NEM + glutathione (1 h incubation; then over column): 109.1

Conclusions:

1. 1h incubation of thrombin with NEM did not appear to result in NEM binding thrombin (sample 3 vs. sample 2).
2. Following ON incubation of NEM with thrombin, some NEM appears to be bound to thrombin, as counts in sample 5 are higher than in sample 4. Maybe thrombin degradation in  $\text{PO}_4$  buffer occurs with time, freeing up -SH groups.

**Blocking of Thrombin and YopM with NEM followed by crosslinking with SMCC**

100  $\mu\text{l}$  of YopM (10 mg/ml) or Fenton thrombin (8.3 mg/ml;  $\pm$  0.1%PEG) were blocked with 0.001 M NEM in 1 ml 0.1 M  $\text{PO}_4$  buffer (pH 7) for 2 h, at RT. After incubation, the samples were concentrated to <75  $\mu\text{l}$  with Centricon-10 filters and run over Bio-Spin 6 columns. The column flow-through samples were used in crosslinking experiments following the protocol described for all other crosslinking experiments.

Results: crosslinked YopM-thrombin product was obtained if one or both of YopM and thrombin were previously treated with NEM.

### Conclusions (speculations!):

1. We wondered if the reactive group on SMCC can displace bound NEM, as the same chemistry is involved in its crosslinking as in that by NEM. Otherwise:
2. The SH group involved in crosslinking YopM and thrombin is not accessible to NEM in the non-complexed proteins (i.e., the YopM-thrombin interaction causes a conformational change in YopM or thrombin that unmasks the crosslinkable SH).
3. We didn't use a high enough concentration of NEM to block SH in these two proteins, even though the protocol we used was a standard one.

### **Preincubation of YopM and thrombin-FPR followed by blockage with NEM and crosslinking with SMCC and DSS**

We had previously shown (33) that YopM binds better to thrombin that has its catalytic site blocked with the tripeptide FPR than to non-blocked thrombin (based on amount of crosslinked product obtained). We used this thrombin to increase the steady-state amount of YopM-thrombin complex that would be present in solution. Then we added NEM after complexes were allowed to form (instead of as a pretreatment as in the previous tests). If there was a conformational change that exposed SH in the complex, those SH could now be blocked by NEM and would not be available for subsequent reaction with SMCC. YopM and thrombin-FPR were preincubated for 30' at RT followed by blockage (or not: control) with NEM (0.001M; 2h at RT). The samples were run over Bio Spin-6 columns and 5  $\mu$ M amounts of the protein mixtures were crosslinked with SMCC or DSS (5 mM; 40 min at RT). The reactions were stopped with 1 M Tris (pH 8) and examined for crosslinked products by western blot using YopM antibodies.

Results: There was no effect of NEM treatment on the amount of SMCC-crosslinked product obtained.

Conclusion: This test did not support the hypothesis of a conformational change in the YopM-thrombin complex that unmasks SH that react subsequently with SMCC.

We did not pursue this quest further and now conclude that Kajava's model is not supported by our data. Currently, we are mutating YopM's third C (to make the C313S YopM). That is the last site-directed mutation we plan to make efforts to formulate molecular models for the YopM-thrombin interaction. That information, together with the other findings of Aim 2 will be written up for publication in a collaborative paper with Andrey Kajava, who will supply molecular modeling for the updated sequences of YopM and the YopM $\Delta$ LRR proteins.

### Final characterization of mutant YopMs prior to testing importance of thrombin-binding in plaque

Rationale. Our goal was to identify a small deletion that abolishes thrombin-binding without grossly deranging the protein and then to

move this mutation into *Y. pestis* and test virulence. If virulence was not changed by the mutation, this would disprove the hypothesis that thrombin-binding is YopM's main function in virulence. If such a *Y. pestis* YopM $\Delta$ LRR mutant was as avirulent as is YopM- *Y. pestis*, this would be consistent with the hypothesis or alternatively indicate that whatever other function YopM has in vivo, it requires regions of YopM in common with that needed for thrombin-binding. We had not obtained a mutant YopM that was clearly defective in thrombin-binding. However, we felt that we might gain useful insight about YopM's function by measuring virulence of *Y. pestis* carrying a  $\Delta$ LRR mutation.

Initially, we chose to test the  $\Delta$ LRR4-7(4-9)yopM mutation, but found that in *Y. pestis* KIM (Pla<sup>+</sup>), this protein appeared to be only weakly expressed, in contrast to when it was expressed from a multicopy plasmid in the Pla<sup>-</sup> *Y. pestis* KIM8-3233. This suggested the possibility that this YopM is susceptible to proteolysis by Pla. We tested this idea by adding YopM $\Delta$ LRR4-7(4-9) to a culture of *Y. pestis* KIM5 and assaying it by western blot before and after the incubation.

**Test for susceptibility of YopM $\Delta$ LRR4-7(4-9) and other YopM $\Delta$ LRR proteins to degradation by surface protease(s) of *Y. pestis* KIM.**

*Y. pestis* KIM5-3233 (Pla<sup>+</sup> YopM<sup>-</sup>) was grown in the defined medium TMH (73) lacking Ca<sup>2+</sup>. The culture was grown at 26°C until an A<sub>620</sub> of 0.5 - 0.6 was reached. At this point the cultures were moved to a waterbath at 37°C and 1 or 0.1 mg of purified intact YopM or YopM $\Delta$ LRR4-7(4-9) was added to the cultures, which were incubated for 5 more hours. Proteins in the cell-free culture media were precipitated with 10% TCA on ice, and the pelleted proteins were resuspended in electrophoresis sample buffer. Samples were analyzed by western blot using YopM antibody. The amounts of YopM and YopM $\Delta$ LRR4-7(4-9) were compared to those of the purified proteins not added to cultures.

Results: YopM remained mostly intact while YopM $\Delta$ LRR4-7(4-9) was degraded.

Conclusion: YopM $\Delta$ LRR4-7(4-9) has an abnormal configuration that makes it susceptible to proteolysis. This would invalidate any conclusions we might wish to make concerning the role of thrombin-binding in the virulence function of YopM, because decreased virulence could be due to decreased half-life of YopM in vivo. Accordingly, YopM $\Delta$ LRR4-7(4-9) is not an acceptable choice for virulence testing.

We made a similar test for YopMS and the 4 other YopM $\Delta$ LRRs that we studied in detail. These YOPMs were not degraded by being co-incubated with *Y. pestis* KIM5. Accordingly, we chose two mutant YopMs to exchange for the wildtype yopM in *Y. pestis* KIM5: YopM $\Delta$ LRR4-5(4-7) and YopM $\Delta$ LRR7-8(7-10). The former was the least affected in its interaction with thrombin as measured by crosslinking, inhibition of platelet aggregation, and ELISA, and the latter was the most affected.



TO 3. Analyze virulence of a *yopM* *Y. pestis* mutant in which YopM is unable to bind thrombin.

Virulence test for importance of thrombin-binding in plague

Allelic Replacement of *yopM* with  $\Delta$ LRR4-5(4-7) or  $\Delta$ LRR7-8(7-10) *yopM* in *Y. pestis* KIM5.

Isolation of  $\Delta$ LRR4-5(4-7)*yopM* and  $\Delta$ LRR7-8(7-10)*yopM* DNA fragments from pBS15/15-based clones carried in *E. coli* XL1 Blue. Strains were grown in Luria-Bertani broth (11) containing 100  $\mu$ g/ml ampicillin (Ap), and plasmids were isolated by using Qiagen Midi Plasmid isolation Kits (Qiagen, Inc., Santa Clarita, CA). Purified plasmids were cleaved with BsrBI, followed by PstI cleavage. The 1.8 kb fragments containing the mutant *yopM* sequences were purified using the Qiaprep Gel Extraction Kit (Qiagen, Inc.).

Isolation of suicide vector pLD55 ( $Tc^R$ , *lacZ* $\alpha$ ). Suicide vector pLD55 was obtained from B. Wanner (35). This plasmid carries *lacZ* $\alpha$ , allowing for blue-white screening of transformants containing plasmids with inserts, and encodes resistance to tetracycline ( $Tc$ ). This allows for selection for plasmid segregants by resistance to fusaric acid (38). The plasmid was isolated from its *E. coli* host following the same protocol as for the YopM mutants described above. Following purification, pLD55 was cleaved by SmaI and treated with shrimp alkaline phosphatase (Boehringer Mannheim).

Ligation of *yopM* mutant fragments with pLD55 vector followed by transformation of *E. coli* DH5 $\alpha$  ( $\lambda$ pir) with ligation mixtures. Mutant *yopMs* were cloned into the SmaI site of pLD55 and transformed into *E. coli* DH5 $\alpha$  ( $\lambda$ pir) using the frozen storage-based transformation protocol described by Hanahan et al. (36). White colonies on Tryptose Blood Agar (TBA; Difco Laboratories, Detroit, MI) plates containing Ap and X-Gal were picked and grown on media containing 15  $\mu$ g/ml  $Tc$  and checked for mutant *yopM* genes by PCR and plasmid mini-preps. Expression was determined in whole cells by western blot using YopM antibodies raised in rabbits.

Allelic exchange of mutant *yopM* fragments with intact *yopM* in *Y. pestis* KIM5 Electrocompetent *Y. pestis* was prepared as previously described (37). Purified plasmid DNA was electroporated into these cells and possible transformants selected on TBA+Ap plates. These colonies were streaked for purity on TBA+Ap followed by selection on TBA+ $Tc$  plates. Potential clones were purified once, nonselectively, on TBA plates and were examined by PCR to ensure that they carried the ~800 bp *yopM* fragment. Clones were then streaked onto "tetracycline-selective agar" (35,38) as a counterselection step and the plates incubated at 30°C for 5-7 days to allow growth of isolates in which a second cross-over had occurred. This counterselection medium was made as follows.

#### **Tetracycline-selective medium recipe.**

900 ml of TBA was supplemented with 25 mg chlortetracycline (Sigma) and autoclaved; 5 g  $\text{NaH}_2\text{PO}_4 \cdot \text{H}_2\text{O}$  in 100 ml  $\text{H}_2\text{O}$  was autoclaved separately and added to the TBA after cooling to 45°C, along with 6 mg of fusaric acid (Sigma) dissolved in 1 ml dimethyl formamide and 2.5 ml of sterile 10 mM  $\text{ZnCl}_2$ .

A final non-selective growth step on TBA was done, and clones were checked for mutant DNA by PCR and for mutant YopM protein production by western blot on culture. Clones were also streaked onto TBA+Tc to ensure that the vector had been lost.

#### **Results and discussion -- virulence of *Y. pestis* $\Delta\text{LRRyopM}$ mutants in BALB/c mice.**

**Table 9. Virulence of  $\Delta\text{LRRyopM}$  mutants in BALB/c mice**

<b><u><i>Y. pestis</i> KIM5 strain</u></b>	<b><u><math>\text{LD}_{50}</math></u></b>
Parent	$4 \times 10^1$ <sup>a</sup> , $< 10^1$ <sup>b</sup>
YopM $\Delta\text{LRR4-5}$ (4-7)	$1.7 \times 10^3$
YopM $\Delta\text{LRR7-8}$ (7-10)	$1.0 \times 10^5$
3233 (YopM <sup>-</sup> )	$3 \times 10^5$ <sup>a</sup> , $7 \times 10^2$ <sup>b</sup>

a = reference 2.  
b = reference 16.

We measured the intravenous  $\text{LD}_{50}$  of *Y. pestis* KIM5 expressing YopM $\Delta\text{LRR4-5}$ (4-7) or YopM $\Delta\text{LRR7-8}$ (7-10) in 6-8 week female BALB/c mice as previously described (16). Table 9 shows the results and, for comparison, includes data for the KIM5 parent strain and for the YopM<sup>-</sup> *Y. pestis* KIM5-3233 from a previous study completed in 1990 (2). The  $\text{LD}_{50}$  values for these strains have varied significantly the two times this was measured. As far as we are aware, there have been no methodological differences in the two studies. In each study, the values were confirmed either by a replicate test(s) and/or by other tests (such as infection timecourse) for which the design was based upon the  $\text{LD}_{50}$  value. The present study found greater virulence for both the parent strain and the YopM<sup>-</sup> mutant (ca. 40-fold decrease in  $\text{LD}_{50}$  for the YopM<sup>-</sup> strain) than was the case in reference 2. This underscores the need to consider only large changes (several orders of magnitude) in  $\text{LD}_{50}$  as significant when small numbers (groups of 5) mice are used. Our  $\text{LD}_{50}$  values are crude estimates; nonetheless, within the same study and between some of our studies over the years, they have had predictive value (e.g., bacteria given at a dose 10-fold below the  $\text{LD}_{50}$  dose were cleared by mice and a dose 10-fold above the  $\text{LD}_{50}$  killed the mice). The loss of YopM caused a modest to moderate decrease in virulence (between 750-fold and ca. 175-fold increase in  $\text{LD}_{50}$ , the latter depending on the actual  $\text{LD}_{50}$  of the parent strain in the present study [Ref. 16]). The YopM $\Delta\text{LRR7-8}$ (7-10) mutant was as avirulent as a YopM<sup>-</sup> strain. The YopM $\Delta\text{LRR4-5}$ (4-7) strain was not as decreased in virulence; but one could argue that it still falls within the range of

virulence shown by a YopM<sup>-</sup> mutant. Accordingly, the interactions of the mutant YopMs with thrombin as measured by the platelet aggregation inhibition assay did not correlate well with the virulence effects of the mutations, as the mutant YopMs both interacted with thrombin approximately as well as did wildtype YopM. Crosslinking was an even poorer predictor of effect of the  $\Delta$ LRR mutations on virulence, because a mutant that crosslinked to thrombin as well as wildtype YopM did (YopM $\Delta$ LRR4-5[4-7]) still was decreased in virulence. This argument would conclude that defects in YopM's interaction with thrombin are not the main virulence-related consequence of the mutations, but rather, some other function of YopM was crippled by the deletions of LRRs. Nonetheless, it is intriguing that the extent of virulence decrease did parallel the (statistically not significant) extent of defect in interaction with thrombin, and it is possible (but not proven by this study) that the difference in virulence of the two mutants is significant.

To satisfy the third deliverable of the Collaborative Agreement, we supplied DNA encoding YopM $\Delta$ LRR7-8(7-10) on a suicide vector with an Ap-resistance marker to Col. Friedlander's research group USAMRIID. We cloned a 1790 bp insert having BsrB1-generated blunt ends into the SmaI-cut (also blunt) pWM91 suicide vector (35), giving a total plasmid size of ca. 10.1 kb (8.3 kb from pWM91 and 1.8 kb insert). We do not know the orientation of the insert in the plasmid (this is immaterial for use of the construct in allelic exchange). There are 584 yopM bp upstream of the  $\Delta$ 7-8 mutation and 310 bp of yopM downstream of the mutation (the rest of the insert, 500 bp upstream and 310 bp downstream, came from a pBR322-derived smaller vector [pBS15/15] from which we cut out the insert to clone into pWM91. Essential features for use of this plasmid in virulent *Yersinia pestis* are that its origin is R6K $\gamma$ , and hence it will be stably maintained only in hosts carrying the  $\lambda$ pir gene (and hence not in *Y. pestis*). It carries the bla gene for ampicillin-resistance selection of first-crossovers and no other drug-resistance genes. The sacB gene provides a modest selection (sucrose-sensitivity) for obtaining second crossovers; however, in our experience this provides a small vs. large colony discrimination, so a large number of colonies still may have to be screened for ampicillin-sensitivity after allowing several days of continuous growth without ampicillin-selection to permit second crossovers to occur.

### Aim 3. Determine the fate of YopM when *Y. pestis* interacts with phagocytic cells.

To 1 and 2: Fate of YopM when *Y. pestis* attaches to the surface of a phagocyte and when *Y. pestis* is engulfed by a phagocyte.

Rationale. To obtain information on YopM's virulence mechanism we needed to identify where YopM localizes when *Y. pestis* infects a macrophage or other eucaryotic cell.

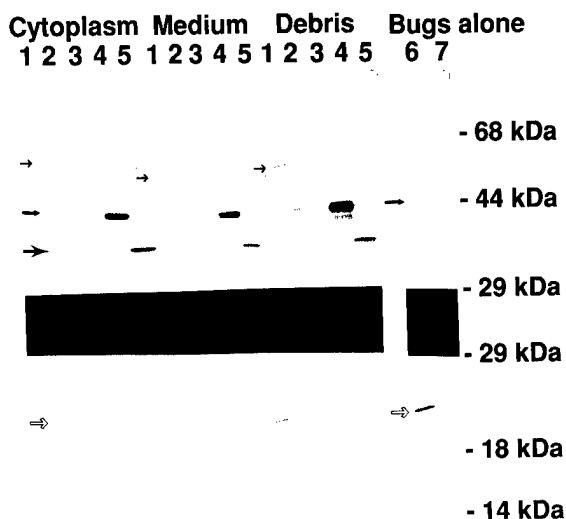
YopM translocation in vitro: yersiniae and antibodies. For our studies of the fate of YopM expressed by yersiniae bound at the eucaryotic cell surface, we created a set of *Y. pestis* KIM strains that vary in their strength of YopM expression (by having an insertion mutation in *yopM* and thereby being YopM<sup>-</sup> or by being YopM<sup>-</sup> and having *yopM* overexpressed (YopM<sup>++</sup>) from its own promoter on the multicopy YopM-overexpressing plasmid pBS10 [3; hereforth called pYopM]). A further level of overexpression (YopM<sup>+++</sup>) can be achieved with pYopM in YopM<sup>+</sup> *Y. pestis*, but we haven't needed this so far. We have the YopM<sup>-</sup> mutation and pYopM in both Pla<sup>+</sup> *Y. pestis* KIM5 and the Pla<sup>-</sup> derivative *Y. pestis* KIM8. The absence of the surface protease allowed us to determine how tightly vectorial *Y. pestis* translocation is by eliminating degradation of Yops released into the extracellular medium. YopE serves as a well characterized reference protein known to be translocated into eucaryotic cells by yersiniae attached at the surface (61,62,66). We have both Pla<sup>+</sup> and Pla<sup>-</sup> strains lacking YopE due to insertional inactivation and the YopE<sup>-</sup> strains carrying YopE overexpressed (YopE<sup>++</sup>) from its native promoter on the multicopy plasmid pYopE that also encodes the SycE chaperone necessary for YopE stability and secretion (this construct was a gift from Greg Plano, U. of Miami).

Vectorial YopM translocation assayed in fractionated mixed cultures.

One way we measure translocation of Yops into eucaryotic cells is by immunoblot analysis of fractions from *Y. pestis*-infected eucaryotic cells. We are using two eucaryotic cell lines, the J774 murine macrophage-like cell and the human epithelial line HeLa. The macrophage is a cell that normally is efficiently invaded by, or actively engulfs, *Y. pestis* (e.g., 59,60,67), and Yops delivery has been shown to inhibit phagocytosis of *Y. pseudotuberculosis* by macrophages (e.g., 65,68). The HeLa cell line has been used extensively in studying Yops targeting by *Y. pseudotuberculosis* (e.g., 61-63,66). We are using this cell line as a reference condition to relate our findings to those already in the literature. We do not know if *Y. pestis* interacts with epithelial cells in vivo.

*Y. pestis* is centrifuged onto J774 or HeLa cells; after a 30 min incubation, nonadherent bacteria are washed out, and the infected monolayer is incubated 2.5 to 4 hours, after which the YopM or YopE distribution is determined by fractionating the culture and carrying out immunoblot analysis. In our initial experiments, we chose the long incubation time of 4 h because periods of 3 to 4.5 h have been used in previous studies (62-64), probably to allow sufficient Yops translocation to occur for easy detection.

Figure 4. YopM and YopE in *Yersinia*-infected HeLa cells. Lanes: 1, *Y. pseudotuberculosis* PB1/+; 2, *Y. pestis* KIM5; 3, Pla<sup>-</sup> *Y. pestis* KIM8; 4, YopM<sup>++</sup> Pla<sup>-</sup> *Y. pestis* KIM8-3233 (pYopM); 5, YopM $\Delta$ LRR4-5(4-7)<sup>++</sup> Pla<sup>-</sup> *Y. pestis* KIM8-3233 (p $\Delta$ 4-5); 6, *Y. pestis* KIM8 in RPMI without HeLa cells, soluble cellular fraction (bacterial cytoplasm + periplasm); 7, culture as in lane 6, cell-free culture medium fraction. Different YopMs are indicated by closed arrows; an open arrow indicates YopE. (The YopM band in medium, lane 1, is diffuse and not visible in the photograph.) Locations of molecular mass markers are indicated at the right.



#### Results and discussion - pilot studies of YopM vectorial targeting using immunoblot as assay

In initial experiments such as illustrated in Fig. 4, yersiniae were grown at 26°C in Heart Infusion Broth, diluted ca. 1:200 into RPMI + 1% FBS, and incubated 2 h at 37°C/5%CO<sub>2</sub> (hereafter called 37/CO<sub>2</sub>) before being added to HeLa monolayers (10<sup>6</sup> cells per dish) at an MOI of 20, centrifuged 5 min at 1,000 rpm, and incubated 30 min at 37/CO<sub>2</sub>. The monolayers were washed 3X and the incubation continued 4 h. Yersiniae alone in RPMI + 1% FBS were similarly incubated. The culture medium was filtered to remove any yersiniae and TCA-precipitated ("medium" fractions). The cells were scraped and lysed in PBS + 0.1% Triton-X-100, which does not lyse *Y. pestis*. After high-speed centrifugation to pellet yersiniae and large debris ("debris" fractions), the soluble cytoplasmic HeLa cell fraction was recovered ("cytoplasm" fraction). Fractions were resolved by SDS-PAGE and transferred to Immobilon-P. The blot was cut, and the upper half was probed with anti-YopM antibody, while the lower half was probed with anti-YopE. After incubation with alkaline-phosphatase-conjugated secondary antibodies, both blots were developed together. Figure 4 and similar experiments showed that *Y. pestis* KIM5 behaves essentially identically to our *Y. pseudotuberculosis* reference strain: all yersiniae injected YopM as well as YopE into the HeLa cell cytoplasm.

Interestingly, both YopM $\Delta$ LRR4-5(4-7) (Fig. 4) and YopM $\Delta$ LRR7-8(7-10) (not illustrated) were vectorially translocated, but we do not know if they function normally once inside. The presence of Pla did not decrease vectorial translocation. In these experiments, we used centrifugation to provide a defined start of infection, but we also can just add *Y. pestis*, and they will adhere and translocate Yops. We do not know what adhesin *Y. pestis* is using.

Figure 4 shows that YopM can be of different sizes in different yersiniae. In the serotype I *Y. pseudotuberculosis* strain PB1/+ shown in Fig. 4, the YopM was significantly larger than that of *Y. pestis* KIM5. YopM of *Y. enterocolitica* O:8 strain WA was of intermediate size. Not all *Y. pseudotuberculosis* strains have the larger YopM: e.g., a serotype III *Y. pseudotuberculosis* has the same size YopM as in *Y. pestis*. We did limited PCR and restriction analysis of the *yopM* genes from these yersiniae and found that it is the LRR-encoding region that is larger than the LRR-encoding region of *Y. pestis yopM* in *Y. pseudotuberculosis* PB1/+ and *Y. enterocolitica* WA. In the case of *Y. pseudotuberculosis* PB1/+, the extra DNA potentially could encode 8 LRRs, giving that YopM 23 LRRs. Given the extent of repeated DNA sequence within *yopM*, it is possible that recombination or slipped-strand mispairing events could give rise to variants with more or fewer LRRs. This could have been responsible for the highly similar LRRs in *Y. pestis* (Fig. 2). It will be interesting to learn the consequences of this variation for YopM function. Perhaps there are sufficient differences in the *yopM* genes of *Y. pestis*, *Y. enterocolitica*, and *Y. pseudotuberculosis* that useful diagnostic probes or antibodies could be generated.

To eliminate Yops secretion into the culture medium by nonadherent yersiniae (see Fig. 4, lane 7), we had to omit FBS during the infection and use yersiniae that had been pregrown at 26°C: thermal induction by pregrowth at 37°C partially overrode the control over Yops secretion in tissue culture medium. The use of 0.1% Triton-X-100 to lyse cells evidently releases a variable but always significant amount of YopM and YopE from the adherent bacteria (which we cannot detach) into the fraction we call the HeLa or J774 soluble fraction. This was assessed by mock-treating yersiniae incubated in wells lacking eucaryotic cells, and it happened with *Y. pseudotuberculosis* as well as *Y. pestis*. This release was significantly decreased by using osmotic lysis with cold water instead of detergent. Only when we were using strains overexpressing YopM or YopE was there significant Yops release from bacteria by water treatment (Fig. 5). We now use brief treatment with trypsin (100  $\mu$ g/ml for 5 min; Sigma) followed by 300  $\mu$ g/ml of Pefablock SC (Boehringer Mannheim GmbH) prior to water lysis to rigorously prevent contamination of eucaryotic soluble fractions by any Yops that might be on the surface of the eucaryotic cell or on the adherent yersiniae (see Fig. 5). The water lysis and vigorous shearing by pipetting to disrupt the cells also disrupts the nuclear membrane as well as the plasma membrane and releases nuclear-localized YopM. Our current handling in Yops translocation experiments is given below.

## Yops distribution by immunoblot of fractionated infected HeLa and J774 cultures -- methods.

HeLa cells are seeded on plates containing six 35 mm wells at a density of  $1-2 \times 10^5$  cells / well in 3 ml RPMI medium (Gibco-BRL) supplemented with 10% heat inactivated fetal bovine serum (RPMI+HIFBS) and incubated for two days at 37° C in the presence of 5% CO<sub>2</sub> (37° C / 5% CO<sub>2</sub>). Cells are washed and covered with 3 ml of warm RPMI medium not supplemented with HIFBS. Cytochalasin D (1 µg/ml; Sigma), colchicine (10 µg/ml; Sigma) and nocodazole (10 µg/ml; Sigma) pretreatments of cells are done for 30 min prior to infection (39). The nocodazole pretreatment involved incubating the cells with the drug on ice for 1 h followed by 30 min at 37° C / 5 % CO<sub>2</sub>. Brefeldin A (Sigma) was added at 10 µg/ml (40), whereas monensin and bafilomycin A1 (Sigma) concentrations were 10 µM and 1 µM (41-43), respectively. Cells are infected to an MOI of 20 by centrifugation of bacteria onto the monolayer for 10 min at 400 x g. After 30 min of incubation at 37° C / 5% CO<sub>2</sub>, unadsorbed bacteria are removed and gentamicin (7 µg/ml) is added if desired. Incubation is then continued in RPMI for 3.5 h with drugs present as above. Next trypsin (100 µg/ml; Sigma) is added to some cultures for 5 min, followed by 300 µg/ml of Pefablock SC (Boehringer Mannheim GmbH). The medium is removed, and the cells are carefully washed with warm phosphate-buffered saline (PBS) and then lysed by vigorous pipetting in 1 ml of ice-cold water containing a cocktail of protease inhibitors (Pefablock, Leupeptin and Pepstatin at 4, 5, and 1 µg/ml, respectively, as suggested by the manufacturer Boehringer Mannheim GmbH). The lysed cells are centrifuged for 20 min at 12,000 x g, and the resulting soluble fraction is precipitated with 10% TCA overnight on ice and resuspended in electrophoresis sample buffer. The pellet of the lysed cells, containing bacteria and large cellular debris, is dissolved in the same volume of SDS-sample buffer. The culture medium is filtered, precipitated overnight on ice with 10% TCA in the presence of carrier proteins (soluble fraction prepared from uninfected HeLa cells), and solubilized in electrophoresis sample buffer. Proteins are separated by SDS-12% (wt/vol) acrylamide PAGE and probed with polyclonal antibodies directed against the whole YopM or YopE molecules. For experiments using J774 cells, the cells are handled as for HeLa cells except that cytochalasin D (5 µg/ml; Sigma) is added 30 min before infection and is present during the incubations with bacteria to prevent phagocytosis of the 26° C-pregrown *Y. pestis*.

Results and discussion - vectorial targeting of YopM assayed by immunoblot

Figure 5. Immunoblot analysis of YopM and YopE in extracts from *Yersinia*-infected HeLa and J774 cells with or without trypsin treatment prior to lysis in water containing a cocktail of protease inhibitors. Cells were infected 4h with YopM<sup>+</sup> *Y. pestis* (wt), YopM<sup>++</sup> *Y. pestis* overexpressing YopM (pYopM) or the YopM<sup>+</sup> YopB<sup>-</sup> *Y. pestis* carrying an in-frame deletion in the yopB gene. All *Yersinia* strains were Pla<sup>-</sup> (to allow detection of any Pla-sensitive YopE in the medium fraction). J774 cells were treated with cytochalasin D (5 µg/ml), added 30 min prior to infection and present during the infection. Proteins were separated by SDS-PAGE, immunoblots were probed with polyclonal antibodies against YopM or YopE, and detection was by alkaline phosphatase-conjugated 2° Abs. Soluble = fraction obtained by water-lysis of infected HeLa cells followed by removal of large debris and adherent yersiniae by centrifugation; proteins were recovered by TCA-precipitation. Medium = culture medium after infection, filtration to remove any bacteria, and TCA-precipitation.

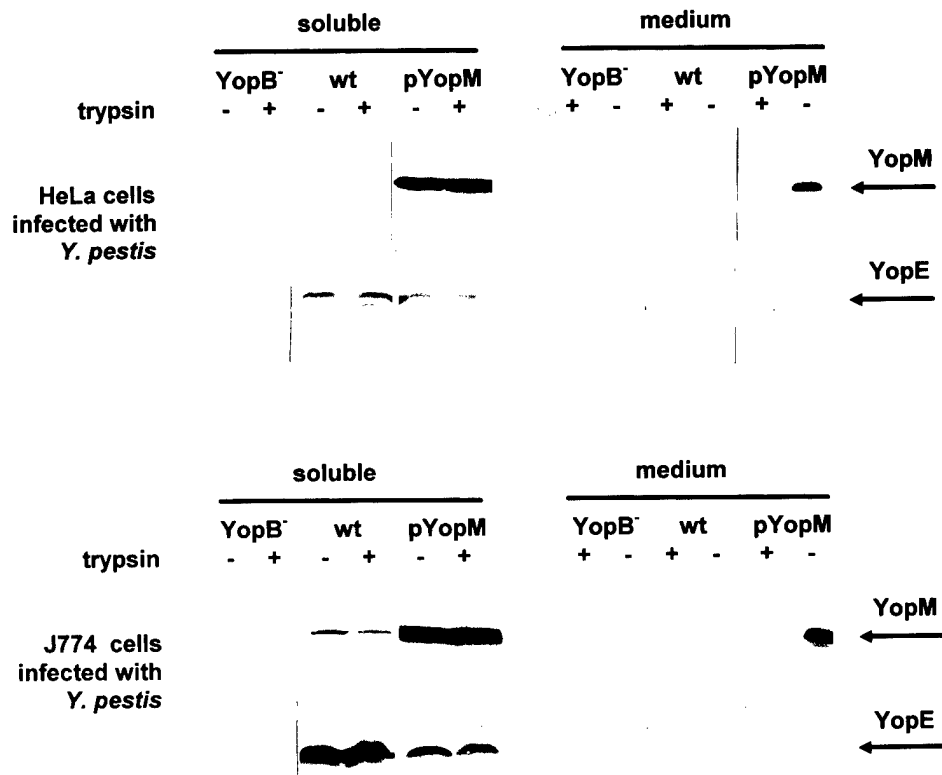


Figure 5 shows that Yops translocation was preferentially into the cell and not into the medium in all cultures infected with yersiniae except those that strongly overexpress their YopM (Fig. 5, pYopM lanes). Overexpression of one Yop apparently overrides the localized



control over secretion (data not shown), and also appears to partially compete with other Yops for access to the secretion machinery (note the lower amount of YopE targeted into HeLa cells in Fig.5, soluble, pYopM vs. wt; data not shown for yersiniae not mixed with HeLa cells). Overexpression is a useful way for us to get enough YopM into the cell for detection at early times after infection, but it cannot be used when the full function of other Yops is important, and it potentially can saturate intracellular targets at longer times after infection. We believe that YopM's work, like that of YopH and YopE, likely is done quickly and when YopM is present in the cell in low amounts. However, without an enzymatic assay for YopM's function (as exists for YopH and recently permitted YopH's action to be studied within seconds after *Y. pseudotuberculosis* adherence [70]), we need initially to amplify amounts of translocated YopM to be able to detect it and its interactions using immunoblots or fluorescence, as indeed was done for YopE and YpkA. As expected (15), Yops targeting required YopB (Fig. 5), and to be polarized, it required the presence of LcrE (not illustrated), in agreement with previous findings (62-64).

The yersiniae were adherent at the surface of the HeLa cells, as treatment of the cells with cytochalasin D (Cyt) to prevent any uptake of the yersiniae did not alter the results (data not shown for HeLa cells, Fig. 5 for J774). To demonstrate vectorial translocation into J774 cells, we had to have Cyt present to prevent phagocytosis, because the Yops antiphagocytic effect is not 100%, and the 26°C-pregrown yersiniae lack their thermally induced antiphagocytic capsule; phagocytosed *Y. pestis*, like intracellular *Y. pseudotuberculosis*, do not translocate Yops.

In an experiment in which the mixed cultures were first incubated 30 min and then, after washing to remove nonadherent yersiniae, gentamicin (7 µg/ml) was added, the appearance of YopE or YopM in the HeLa or J774 cytoplasmic fraction was almost abolished. This also supports the extracellular location of the yersiniae in these experiments, as only extracellular yersiniae are accessible to inhibition by gentamicin (e.g., 61,63,64).

We have recently begun to use more gentle lysis to obtain intact vesicular fractions from infected cells for analysis of their YopM and other protein contents. The Balch homogenizer (69) shears eucaryotic cells gently without the use of detergent and, when properly adjusted, breaks only the plasma membrane, leaving internal vesicles and nuclei intact. The cells are drawn over steel balls, and the size of the balls can be adjusted for the cell line at hand. In a pilot experiment, infected HeLa cells were broken in a Tris-sucrose buffer containing protease inhibitors; large debris (including adherent yersiniae, cell nuclei, other large organelles) was pelleted; and the soluble fraction was further clarified by ultracentrifugation. The resulting cytoplasmic and small vesicle fractions were analyzed for YopM by western analysis. The majority of YopM was in the cytoplasmic fraction, but a significant amount was associated with the small vesicles. This is consistent with our observations by fluorescence microscopy that suggest that YopM is vesicle-associated when in the cytosol (see below). Overexpression of YopM and infection for 4 h in

this experiment likely saturated YopM's trafficking partner, leaving unbound YopM in the cytosol.

YopM distribution by immunofluorescence staining and confocal microscopy of infected HeLa cells. To study the fate of YopM inside eucaryotic cells, we used conventional indirect immunofluorescence microscopy and laser scanning confocal microscopy of HeLa cells infected with the YopM<sup>-</sup> *Y. pestis* KIM8-3233 and its derivative overexpressing YopM. Overexpressed YopE served as a reference protein.

Our current methods for this kind of experiment are given below, followed by a step-wise presentation of our current protocol for immunofluorescence sample preparation.

## Methods for immunofluorescence experiments.

HeLa cells are grown as monolayers to semi-confluence (average  $4-8 \times 10^4$  cells per 12 mm coverslip) in RPMI+HIFBS at  $37^\circ\text{C}$  / 5%  $\text{CO}_2$ . Monolayers were washed and covered with 1 ml of warm RPMI. If required, cells are pretreated with cytochalasin D, colchicine, nocodazole, brefeldin A, monensin and bafilomycin A1 as described above for experiments analyzing Yops translocation by western blot. Taxol (Paclitaxel) (Sigma) is used at  $10 \mu\text{g/ml}$  for 30 min at  $37^\circ\text{C}$  / 5%  $\text{CO}_2$  (75). Cells are infected (MOI of 30), washed with warm medium after 30 min and incubated as described above for western blot analysis. After 2 h or 3.5 h, some cultures are washed with warm PBS and treated for 5 min at room temperature (RT) with digitonin ( $10 \mu\text{g/ml}$  in PBS) (Calbiochem) (44,45), followed by fixation with 2% paraformaldehyde. The samples are permeabilized with 0.5% Triton X-100 in a microtubule stabilizing buffer (66) and optionally treated for 5 min at RT with Hoechst 33342 fluorescent stain ( $5 \mu\text{g/ml}$  in PBS) (Molecular Probes). The specimens are incubated with affinity-purified rabbit anti-YopM antibodies or mouse anti-YopE antibodies followed by Oregon Green-conjugated secondary antibodies (Molecular Probes). The arrangement of microtubules in uninfected and infected cells is visualized by using anti- $\alpha$ -tubulin antibodies (Sigma). The effect of other drugs perturbing the cell's vesicular system is monitored by uptake (1 h at  $37^\circ\text{C}$  / 5%  $\text{CO}_2$ ) of BODIPY FL-labeled immunofluorescent transferrin ( $20 \mu\text{g/ml}$ ), LDL ( $20 \mu\text{g/ml}$ ), and  $\text{C}_5$ -ceramide ( $5 \mu\text{M}$ ) (Molecular Probes) or by the use of anti- $\gamma$ -adaptin antibodies (Transduction Laboratories) followed by secondary Oregon Green-coupled antibodies. Coverslips are mounted using Vectashield mounting medium (Vectors Labs, Inc.) and examined with a Zeiss Axiophot microscope with epifluorescent illumination and a 40x (NA 0.75) objective. Optical scanning currently is done using a laser-scanning confocal microscope equipped with an argon-krypton laser (Multiprobe 2001 Molecular Dynamics) and an inverted microscope (Diaphot, Nikon) using 40x (NA 0.95) or 60x (NA 1.4) Apochromat objectives. Sets of fluorescent images are visualized in pseudocolor to represent different intensities. White, red, yellow colors indicate maximal and progressively lower fluorescence intensities, respectively, corresponding to the highest level of YopM or YopE targeting, whereas blue and dark colors represent low and minimum intensity and show the absence of specific staining. For each treatment of cells infected with pYopM or pYopE strains adjustments are made not to get a nonspecific signal from the corresponding treatments of YopM or YopE controls. Optical sections are scanned in  $0.5 \mu\text{m}$  steps (25 sections with image size  $512 \times 512$ ), giving a pixel size of  $0.21 \mu\text{m}$  (60x objective) or  $0.32 \mu\text{m}$  (40x objective).

## Immunofluorescence Sample Preparation

For each treatment, seed duplicate 12 mm coverslips in a 24-well cluster dish with HeLa or J774 cells and use at semi-confluence (average 4 to 8 x 10<sup>4</sup> cells per 12 mm coverslip).

In all handling below prior to mounting on microscope slides, the coverslip remains in the dish, and solutions are added gently down the sides of the wells and gently removed with an aspirator or Pipetman.

1. Wash at least 3X with warm PBS, ca. 1 ml per wash.
  - a. Optional digitonin treatment:  
just-cover the coverslip using 0.5 ml room-temperature (RT) digitonin;  
incubate 5 min RT.  
We use digitonin at 10 µg/ml in PBS for HeLa cells; this concentration has to be optimized for each cell type. Digitonin stock is 40 mg/ml in PBS and is stored frozen. Thaw and remix just before use.
  - b. Remove digitonin and wash twice with 1 ml/wash of RT PBS.
2. Fix 15 to 60 min at RT with 0.5 ml 2% (wt/vol) paraformaldehyde (made in PBS; pH 7.2 to 7.6).  
Paraformaldehyde is freshly diluted from 4% stock in PBS (pH 7.2-7.6).  
Recipe for stock is below.
3. Wash coverslips at least 3 times with 1 ml RT PBS.
4. Permeabilize cells 10 to 15 min at RT with 0.5 ml 0.5% (wt/vol) Triton X-100 in microtubule-stabilizing buffer (100 mM PIPES pH 6.9, 4% PEG 6000, 1 mM EGTA).
5. Wash coverslips 2 to 3X with 1 ml RT PBS/wash.
6. Optional: Treat for 5 min at RT with 0.5 ml Hoechst 33342 (5 µg/ml in PBS) or other chromatin stain (as for FACS).
7. Wash coverslips 2 to 3X with 1 ml RT PBS/wash.
8. Block 1 h at RT with 0.5 ml 10% heat-inactivated FBS in PBS containing 1% mouse serum (if 1° antibody is rabbit; rabbit serum if 1° is mouse; to block surface FcR).
9. Wash coverslips 2X with 1 ml RT PBS/wash.
10. Treat coverslips 1 h with 0.2 ml 1° antibody diluted in PBS containing 1% mouse/rabbit serum (1° antibody typically is relatively concentrated, such as 1:100 to 1:400 dilution of antibody -- dilution has to be determined empirically for each antibody).

## Immunofluorescence Sample Preparation -- cont'd

11. Wash coverslips at least 3X with 1 ml RT PBS/wash.
12. Treat coverslips 1 h with 0.2 ml fluorochrome-coupled 2° antibody diluted in PBS containing 1% mouse/rabbit serum (commercially available antibody such as goat anti-rabbit IgG (whole molecule) coupled to Oregon Green; diluted as suggested by manufacturer -- e.g., 1:100 to 1:200; however, best to check dilutions of it for optimal dilution).
13. Wash coverslips 3X with 1 ml RT PBS/wash.
14. Drain excess liquid from coverslips but do not dry; invert and mount using Vectashield (Vector Labs, Inc) or other (e.g., Molecular Probes) mounting medium. Seal with clear nail polish (Kroger).
15. Store in the dark at 4°C.
16. Check staining with conventional epifluorescent microscope; then do confocal, adjusting settings to eliminate nonspecific noise from negative control while preserving signal from experimental samples.

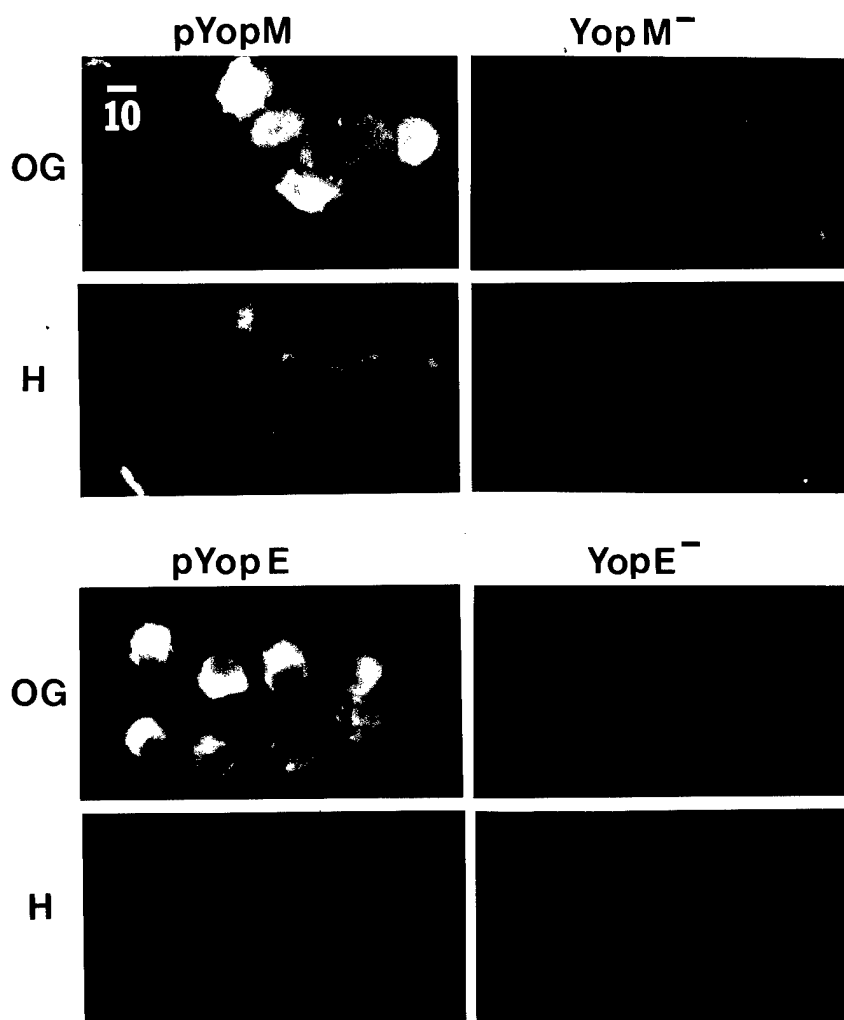
### 4% paraformaldehyde

In < 50 ml water, add 4 g.  
Warm 20 min at 60°C  
Titrate solid into solution with NaOH (e.g., 5N)  
Titrate back to pH 7.2-7.6 with HCl  
Make to 50 ml with water  
Add 50 ml 2X PBS

Wrap bottle with Al foil and refrigerate. Stock can be stored for at least 2 weeks, and maybe 1 to 2 months (according to one protocol we have -- but check its pH).

Results and discussion - YopM localization within eucaryotic cells after vectorial targeting by *Y. pestis*

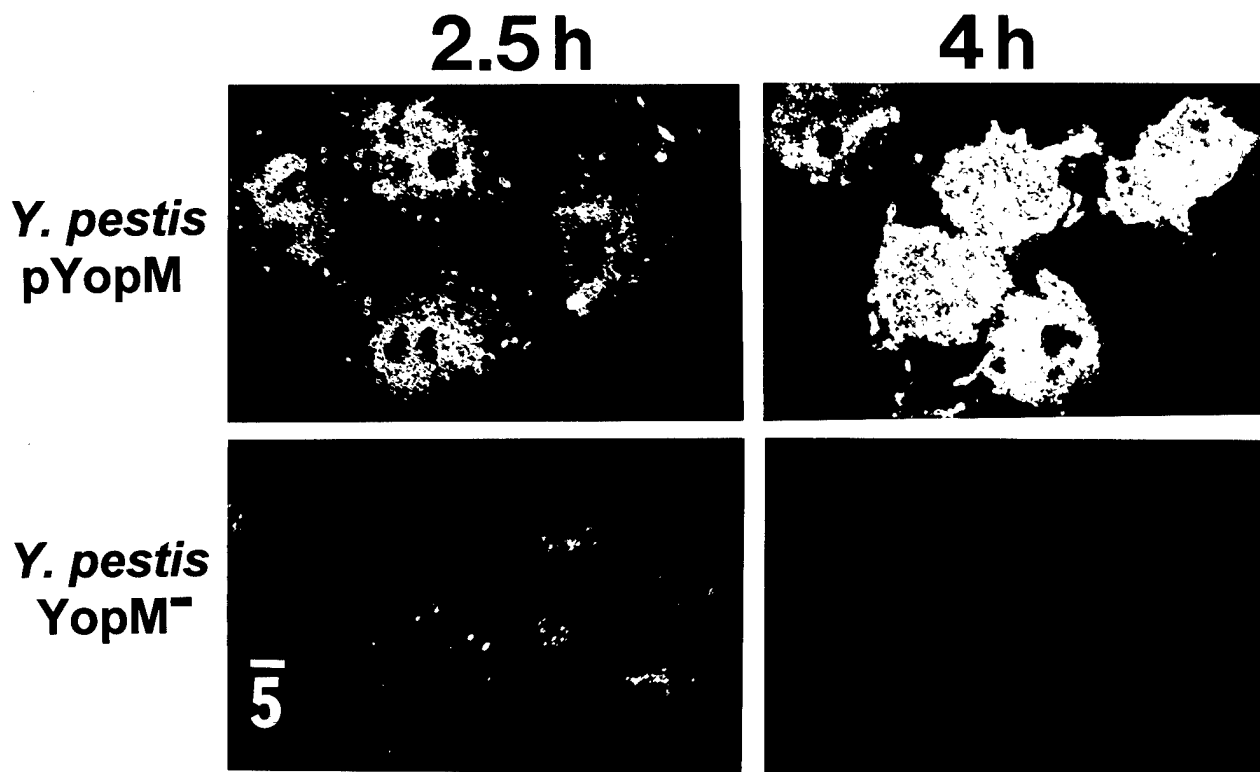
Figure 6. Distribution of YopM and YopE within infected HeLa cells. HeLa cells were infected with *Y. pestis* KIM8-3233 (pYopM) and KIM8-3122 (pYopE) or their YopM<sup>-</sup> or YopE<sup>-</sup> counterparts. Specimens were double stained with anti-YopM or anti-YopE antibodies followed by secondary Oregon Green-conjugated antibodies (OG), and with chromatin-specific Hoechst 33342 stain (H). Samples were examined by conventional fluorescent microscopy. The bar equals 10  $\mu$ M. The yellowish color of pYopM-OG or pYopE-OG samples, comparing with the green color of YopM<sup>-</sup> or YopE<sup>-</sup> controls indicate specific staining.



All of our strains, with the exception of the YopB<sup>-</sup> and YopD<sup>-</sup> mutants, caused cytotoxicity, presumably due to the effects of targeted YopE and YopH; accordingly, the HeLa cells appeared rounded-up. This was

noticeable starting after around 2 h of infection and was strongly exhibited by 4 h. Figure 6 shows that after 4h of infection, YopM was evenly distributed throughout the whole cell, including the nucleus. In contrast, comparison of the distribution of Hoechst stain for chromatin with fluorescence locating YopE showed that YopE was cytoplasmic as previously described (66). (The few cells appearing to be completely filled with YopE probably had YopE-filled cytoplasm overlying the nucleus, but it would require confocal microscopy of those cells to prove this.) Cells infected with YopM<sup>-</sup> or YopE<sup>-</sup> yersiniae remained uniformly dark.

**Figure 7.** YopM localization in the cytoplasm and nucleus of HeLa cells. HeLa cells were infected with *Y. pestis* KIM8-3233 (YopM<sup>+</sup>) or its derivative carrying plasmid pYopM. Cells were infected with bacteria for 2.5 h or 4 h before being processed for YopM detection by indirect immunofluorescence. The samples were optically scanned under identical conditions using a confocal laser-scanning microscope and comparable single optical sections were recorded in pseudocolor. The bar equals 5  $\mu$ m.



When similar samples were analyzed 2.5 h after infection by confocal microscopy, YopM was found in a granular pattern indicative

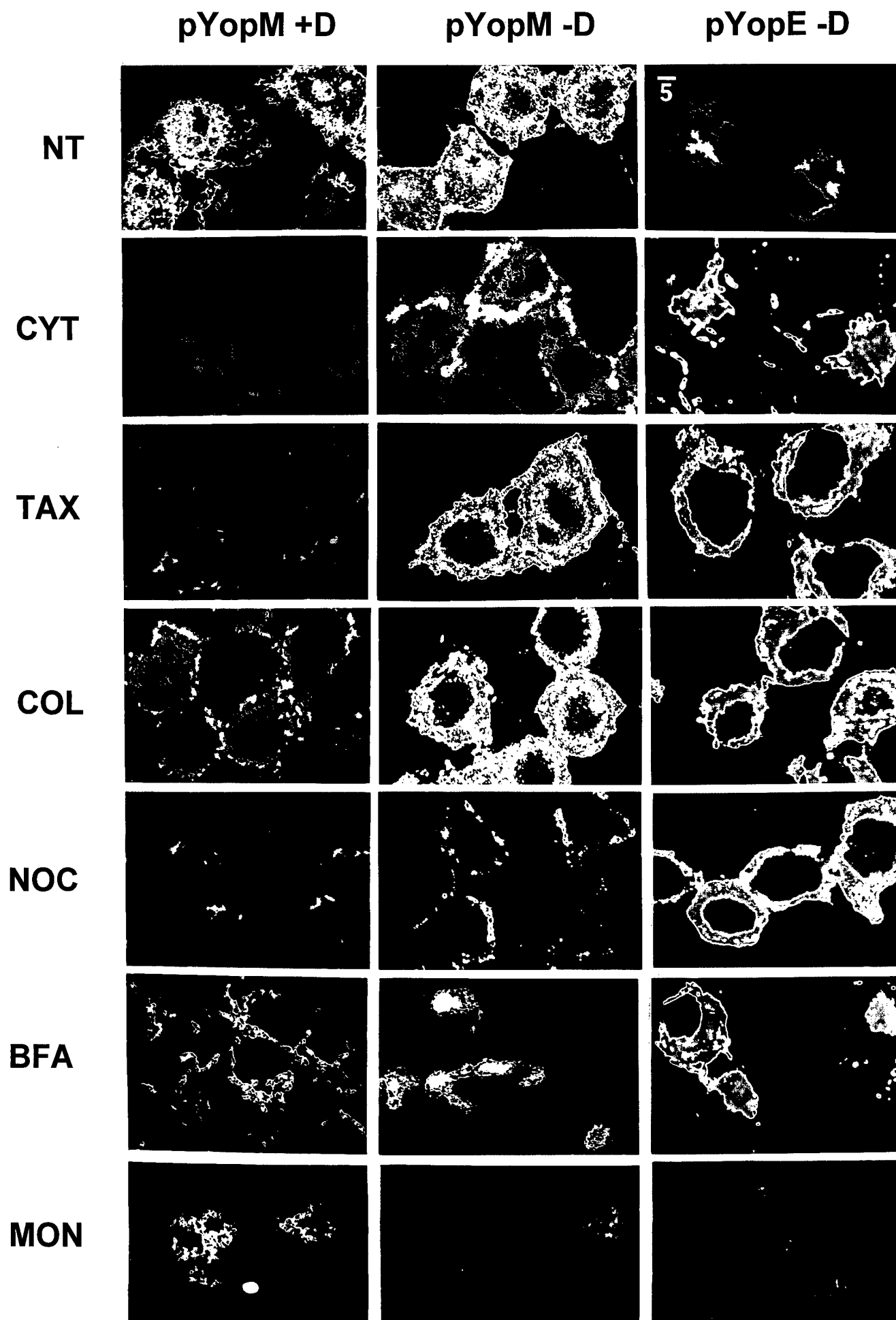
of foci of YopM accumulation (Fig. 7). In some experiments, this punctate character was clearly in the cytosol, suggestive of a vesicular association for YopM. 1.5h later, YopM had clearly accumulated throughout the whole cell, including the nucleus (Fig. 7). There was considerable heterogeneity among cells for YopM's distribution (in contrast to YopE, which was consistently present in its typical perinuclear location): some cells did not fluoresce at all or showed YopM mainly in the cytoplasm and less in the nucleus, whereas others were accumulating YopM in both compartments (Figs. 6, 7, 8). We do not yet understand this but suspect that one factor is heterogeneity of the cell cycle phase within the HeLa cell culture. The ability to detect YopM by fluorescence is affected by the state of the cells, even when immunoblot analysis reveals no variability in the amount of YopM translocated in the overall culture (see later).

#### YopM traffics on the cell's vesicular system.

In search of YopM's intracellular target, we treated HeLa cells with various drugs known to affect cytoskeletal or vesicular structures and infected with *Y. pestis* overexpressing YopM (pYopM) or YopE (pYopE), and with their Yop-negative counterparts (Fig. 8).

**Figure 8.** Effect of cytoskeleton and vesicle-altering drugs on YopM and YopE distribution in HeLa cells. HeLa cells were infected for 4h with *Y. pestis* KIM8-3233 (pYopM), KIM8-3122 (pYopE) and their YopM or YopE counterparts (not shown). The HeLa cells were either left untreated (NT) or treated with cytochalasin D (CYT), taxol (TAX), colchicine (COL), nocodazole (NOC), brefeldin A (BFA) and monensin (MON). Samples were processed for indirect immunofluorescence using antibodies specific for either YopM or YopE. The left-most column shows YopM-specific staining in specimens treated with digitonin (+D), whereas the middle and the right-most columns show cells not treated with digitonin (-D). To illustrate heterogeneity of the YopM distribution within cells, the picture representing HeLa cells infected with the pYopM strain (middle column-NT row) was composed from two separate images from the same specimen. Immunofluorescence was detected by laser scanning confocal microscopy using a 40x (NA 0.95) objective (the left-most column: CYT, TAX, COL, NOC, BFA) or 60x (NA 1.4) objective (all other specimens). Single, comparable optical sections are shown. Fluorescence intensity is represented by pseudocolor. The bar at top, right applies only to the images recorded with the 60x objective; the other images are 1/3 smaller due to the difference in objective used for data acquisition.





None of the drugs affected the translocation of YopM, as measured by immunoblot analysis of the soluble fraction of the drug-treated infected HeLa cells. We used anti- $\alpha$ -tubulin antibody to ensure that the microtubule-altering drugs had their expected effects and BODIPY FL-labeled transferrin, LDL, and  $C_5$ -ceramide or anti- $\gamma$ -adaptin antibodies to confirm the effects of other drugs altering the cell's vesicular system. To better visualize YopM in the nuclei of infected host cells, we exploited the selectivity of the nonionic detergent digitonin for the plasma membrane. When used at a low concentration, digitonin selectively permeabilizes membranes containing a high concentration of  $3\beta$ -hydroxysterols such as cholesterol, which are predominant in the plasma membrane and less so in internal membranes (except for newly formed endosomes) (44,45). We found that treatment with digitonin prior to fixation and permeabilization gave enhanced detection of YopM in nuclei, perhaps by increasing the accessibility of the cell interior to the subsequent fixation and permeabilization treatments. There was no detectable YopM when infected cells were treated with digitonin and fixed without subsequent Triton X-100 permeabilization. In digitonin-treated cells, free or loosely bound YopM in the HeLa cytosol was removed by subsequent washes, and the YopM remaining was mainly associated with a structure that was not permeabilized by digitonin. YopE, in contrast, remained in the cell's cytosol, permanently bound to an unknown structure such that even a high concentration of digitonin (40  $\mu$ g/ml) was not able to remove it.

Cytochalasin D distorted the cellular shape beyond that due to the F-actin depolymerization in response to YopE, but did not qualitatively alter YopM or YopE's distribution within the cytoplasm or YopM's targeting to the cell's nucleus (Fig. 8 CYT). Taxol, which promotes microtubule assembly and inhibits disassembly (Mogensen and Tucker, 1990), caused the formation of parallel arrays of microtubules and multiple asters of stable microtubule bundles independent from the centrosome (data not shown). This appeared to slightly enhance YopM detection in the cytoplasm and promoted its nuclear localization (Fig. 8 TAX). There was no noticeable effect on the amount or distribution of targeted YopE. However, taxol did appear to counteract some of YopE's cytotoxic effect in that the cells were less rounded up than in infected cells not treated with taxol (Fig. 8). Colchicine and nocodazole both bind to tubulin and prevent polymerization of microtubules, and because of dynamic instability of microtubules, cause their depolymerization (39). Colchicine had no significant effect on YopM or YopE distribution in the cytoplasm, whereas the more tubulin-specific nocodazole appeared to have a drastic effect on the amount of YopM but not YopE detectable by immunofluorescence when analyzed in cells not treated with digitonin (Fig. 8 -D column).

(Recall that nocodazole did not affect YopM translocation measured by immunoblot.) This effect disappeared upon digitonin treatment (Fig. 8 +D column), as though YopM was unmasked for reactivity with antibodies when this treatment preceded the regular fixation and permeabilization steps. Nocodazole's YopM-dispersal effect likely includes an effect of the ice pretreatment to depolymerize microtubules, rather than solely a specific effect of nocodazole, as HeLa cells given only the ice pretreatment also showed a diminution in YopM staining (data not

presented). Both drugs caused a decreased amount of YopM to localize in the nucleus. However, YopM's distribution did not correlate directly with that for tubulin (not shown), so we do not think that YopM binds to microtubules. Our data suggest that microtubules are involved in YopM's cytoplasmic trafficking and that they may indirectly promote its targeting to the nucleus.

We tested the dependence of YopM's distribution on vesicular trafficking by using drugs that disrupt the cellular endocytic pathway. Bafilomycin A1, which inhibits the vacuolar H<sup>+</sup> ATPase, and the ionophore monensin both cause alkalinization of vesicles that normally are acidified by active proton transport and treatment with these compounds prevents the fusion of endosomes to the endosomal sorting compartment or further to lysosomes (41-43). In monensin-treated HeLa cells, YopM-specific fluorescence was restricted to peripherally located vesicles, supporting a hypothesis in which YopM's trafficking involves a functional endosomal pathway. However, not all of the YopM was trapped there, because after digitonin treatment, a small amount of this protein was visible in the nucleus, whereas the putative early endosome-associated protein disappeared, perhaps because digitonin disrupted that compartment (Fig. 8 MON). A similar cytoplasmic localization pattern was observed in bafilomycin A1-treated cells; however, there was no inhibition of YopM accumulation in the nucleus, as though bafilomycin's trafficking block was not as strong as that from monensin. Significantly, YopE localization was not affected by either drug, underscoring the specificity of these observations for YopM (Fig. 8). Another vesicle-altering drug, brefeldin A, prevents coatamer assembly by inhibiting the GTP-exchange of the ARF GTPase necessary for vesicle budding in the trans Golgi network (TGN), the endoplasmic reticulum (ER), the Golgi apparatus, and perhaps also in the plasma membrane (40,46-49). As a result, there occurs a disconnection of communication between the endocytic and TGN compartments on the one hand, and the ER and Golgi compartments on the other, and the vesicular system shows extensive morphological changes, including large tubulated endosomes and a dispersed, tubulated Golgi fused with ER. In brefeldin A-treated cells, YopM was present in large elongated bags that extended through many optical sections (Fig. 8, BFA-one 0.5  $\mu$ m section is shown). Importantly, the YopE distribution was not affected by this treatment (Fig. 8), showing that the brefeldin A effect was specific for YopM's trafficking. The appearance of YopM supports the idea that the cytoplasmic trafficking includes a membrane-associated compartment. Treatment with digitonin removed almost all of the YopM and revealed that there was none in the nucleus. The peripherally located fluorescence in digitonin-treated cultures probably was mostly from yersiniae, showing that the YopM-associated compartment in brefeldin A-treated cells was sensitive to digitonin and suggesting that it was of endosomal origin. Since brefeldin A completely abolished YopM's nuclear targeting, it appears that YopM's association with this putative vesicular compartment was irreversible. Our findings indicate that before YopM gains entry to the nucleus, it traffics in association with a vesicular pathway.

Use of digitonin to enhance visualization of YopM in the eucaryotic nucleus The nuclear destination of YopM was an intriguing property. To improve the detection of YopM in the cell's nucleus we exploited the selectivity of digitonin for the plasma membrane. In our hands, a low concentration of this detergent enhanced the visualization of YopM in the nucleus, sometimes dramatically (Fig. 8 +D column). This could have been due to more effective fixation or permeabilization of the nuclear membrane after digitonin treatment; however, we can not exclude that this treatment could release YopM from hydrophobic interactions and unmask additional epitopes, making it more visible for antibodies. When the concentration of digitonin was increased, the nuclear staining of YopM was gradually lost, illustrating the need for a low concentration to have selectivity of the digitonin treatment. No detectable YopM was found in the cells treated with digitonin only or additionally fixed but not permeabilized, or in noninfected cells or cells infected with YopM *Y. pestis*, that were treated with digitonin and processed alongside the infected cultures. This reassured us that the observed enhancement in detection was specific for YopM. YopE remained tightly bound to an unknown structure, because even high concentrations of digitonin and two washings did not wash it out from the cell's interior.

#### Site-directed mutagenesis of KDEL-like sequence

YopM's C-terminus ends in the sequence DKLEDDVFE. This DKLEDD stretch bears some similarity to the "KDEL" sequence that operates to return RER proteins to the RER from the Golgi and that is used by some toxins for retrograde transport (47). To test whether this sequence is important for YopM's distribution within eucaryotic cells, we mutated this sequence, by the method described previously for LRR deletions and C-to-S mutations, to DAALEDD. The primers, shown below, changed a nearby *NdeI* site to a *SunI* site without changing the encoded amino acids. Underlined bases are mutagenic bases; italicized, small-font bases specify the *SunI* site; bolded large-font bases specify the alanine replacements.

#### **Primers for the site-directed mutagenesis**

##### pKDELup

*SunI*

5' AGT TAG CCG TAC GAA TTT GCT CAT GAG ACT ACA GAC **GCA GCT** GAA GAT

K402A L403A

GAT 3'

##### pKDELdown

*SunI*

5' GAC GTG TTC GTA *CGG* ATC AAC TAC ACG TTC CGA GTT CAT 3'

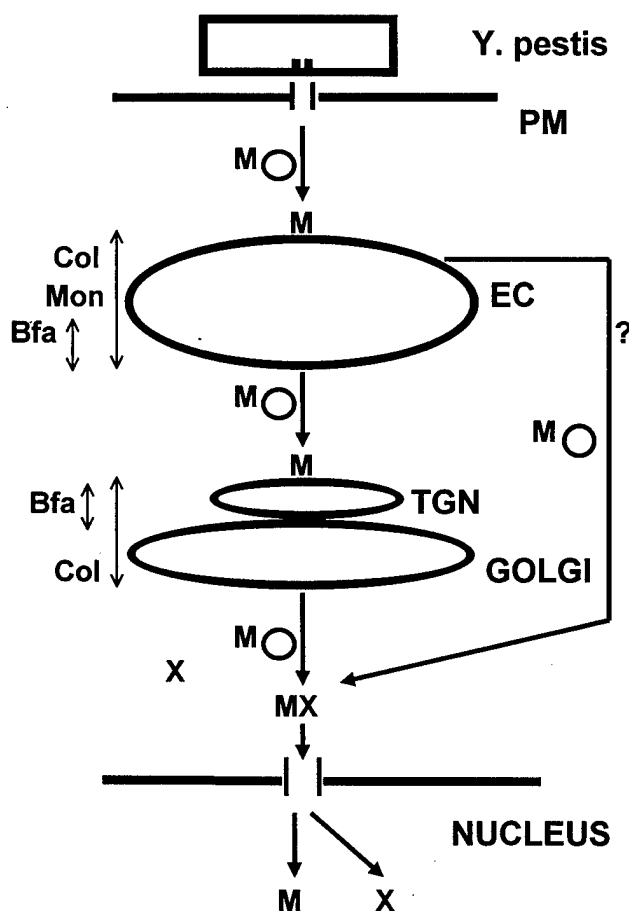
#### Results and discussion - "KDEL" mutant YopM

The resulting mutant YopM was secreted somewhat more weakly than is wildtype YopM, but it appeared to localize normally within eucaryotic cells. This indicates that YopM does not need this C-terminal

sequence for its trafficking and is consistent with the idea that YopM does not bind to a KDEL receptor, which would require ligand-receptor interaction within the lumen of vesicles.

#### Model for YopM's movement within eucaryotic cells

**Figure 9.** Working model for YopM's cellular trafficking. YopM (M) enters the cell through a putative pore in the plasma membrane (PM) and binds to the surface of a vesicle which then carries YopM to the endosomal compartment (EC). YopM's endosomal trafficking is microtubule-dependent and affected by colchicine (Col), monensin (Mon), and bafilomycin A1 (Bfa). Alkalinizing drugs like monensin (Mon) and bafilomycin A1 cause YopM to accumulate in this compartment. Brefeldin A (Bfa) could prevent YopM from leaving the EC. If YopM reaches the trans Golgi network (TGN), brefeldin A (Bfa) also would prevent YopM from leaving this compartment. At some point, YopM is released from the surface of the vesicle and interacts with the hypothetical component X, which chaperones YopM through the nuclear pore.



In our model, YopM enters the cell's cytosol from the surface-located *Y. pestis* directly through the hypothetical pore created by YopB and YopK (Fig. 9). Since there is no evidence for Yops delivery in *Yersinia* via coated or uncoated vesicles formed at the contact zone between bacteria and eucaryotic cell, we propose that YopM flows directly into cell's cytosol instead being engulfed into an endocytic vesicle. This conservative hypothesis also is based on the assumption that YopM is delivered into cells in the same matter as is YopH, which finds its cytosolic targets within seconds (50). Next, YopM binds to the surface of an early endosome, which can fuse with other vesicles further in the endosomal pathway. This pathway ultimately transports YopM to the surface of a compartment where it meets its nuclear trafficking partner. In contrast, YopE apparently moves to its target without any dependence on vesicular elements and remains associated with an unknown structure, a process that makes this protein insensitive to any of our drug treatments. We cannot exclude that some YopM remains unbound, particularly after long infection times when specific YopM interactions could have been saturated by the large amount of YopM present. However, brefeldin A completely blocked YopM from entering the nucleus even after a long infection time. The efficiency of YopM's trafficking may depend more on the function of microtubules than microfilaments, as it was decreased by colchicine or nocodazole / cold treatments, enhanced by taxol, and not much affected by cytochalasin D. We propose a vesicular association for YopM because of the punctate appearance of YopM's early distribution (Fig. 7), and because vesicle-alkalinizing drugs like monensin and bafilomycin A1 were able to alter YopM's intracellular fate. Colchicine's diminution of the amount of YopM reaching the nucleus is also consistent with preferential role of carrier vesicles over a passive flow of YopM in the cell. Monensin, like bafilomycin A1, restricted YopM to a peripheral location, reminiscent of its effect on trafficking of diphtheria toxin in Cos cells (41); significantly, this cytoplasmic YopM disappeared after treatment with a low concentration of digitonin (Fig. 8), consistent with the interpretation that alkalinizing drugs restrict YopM's vesicular association to early endosomes. In brefeldin A-treated cells, YopM may be associated with a large tubulated endosomal compartment (EC) rather than a dispersed fused Golgi / endoplasmic reticulum (ER) compartment, because of the morphology of the YopM pool (large bags rather than a highly tubulated network). We speculate that in brefeldin A-treated cells YopM is trapped in association with a compartment where it accumulates but can not escape. This compartment, if vesicular, could have been altered in its surface by brefeldin A, e.g., by lacking  $\beta$ COP or clathrin (40,47), and as a result be enhanced in its strength of binding YopM. In contrast, in monensin or bafilomycin A1-treated cells, where the coat formation on new vesicles is not disturbed, some YopM still traffics to the nucleus. Because of the transient nature of coat structures (47) and our finding that brefeldin causes YopM to concentrate in a discrete compartment rather than to disperse through the cell, we do not believe that YopM binds coats directly. We speculate that vesicle-bound YopM reaches the TGN, because YopM piles up in a compartment behind the brefeldin A block, and brefeldin A has

long been known to set up a block between the TGN and Golgi. However, because of more recent evidence that brefeldin A also blocks movement out of the EC (49,51), our data do not rule out the possibility that YopM bypasses the TGN. We do not know if YopM is retrogradely transported to the ER: it lacks motifs associated either with retention in a vesicular compartment or promotion of transport within the ER and Golgi vesicular pathways (47). Lack of a role of the Golgi apparatus in YopM localization is suggested by the absence of a qualitative effect of colchicine on YopM distribution (colchicine, like nocodazole, causes the Golgi to fragment and disperse [52]). We propose that on its journey through the cell, YopM subsequently becomes associated with a protein that releases it from its membrane-associated carrier and chaperones it through the nuclear pores. This hypothetical nuclear trafficking partner (marked X in Fig. 9) must be absent from the hypothetical vesicle that YopM accumulates on in brefeldin-treated cells, or it is unable to compete with YopM's binding to this vesicle. We propose a nuclear transport partner for YopM, because there is no instance known of nuclear delivery via vesicles (47), and YopM does not contain a sequence resembling one of the known nuclear localization signals (NLS) for the regulated entry via nuclear pores (52-55). Since YopM is of a size that would diffuse only slowly through the pores (54), we speculate that YopM is actively transported by a partner containing a NLS, rather than by passively diffusing through the nuclear pore.

#### Significance of YopM's nuclear localization

YopM's trafficking to the nucleus places it as only the third bacterial virulence protein known to do so and the only one lacking a consensus NLS: the  $\alpha$ -protein cleaved from *Neisseria* IgA1 protease has a NLS and localizes to nucleolus (56), and VirD2, which has also a NLS, carries *Agrobacterium* T DNA into the nucleus (57). The avirulence protein AvrBs 3 of *Xanthomonas campestris* pv. *vesicatoria* has a NLS which is required for it to cause the hyper-sensitive response, making that protein another one that likely is transported into the host cell nucleus (58). We speculate that once YopM is in the nucleus, it binds a nuclear target and exerts its pathogenic effect. Future studies will show whether YopM manipulates host gene expression responsible for a protective immune response. YopM yersiniae are normal in their growth in liver and spleen until day 3 or 4 in a mouse model of systemic plague (2); then their growth is curbed and the bacteria are subsequently cleared. Perhaps it is this infection-elicited, growth-curbing host response that is undermined by YopM's activity in the nucleus.

We have shown here an intracellular trafficking and destination of one of the *Y. pestis* targeted proteins, YopM. We believe that the further study of the mode of action of this protein in host cells will provide insight into both bacterial pathogenesis and mammalian cell biology.

## Conclusions

### Aim 1. Assess the immunogenicity and protective capacity of YopM.

- YopM is expressed during plague in humans and elicits an antibody response. This response could be useful diagnostically, particularly if plague-specific probes can be designed based on unique sequences in *Y. pestis yopM*.
- YopM is not a protective antigen for inbred or outbred mice immunized passively with either mouse or rabbit anti-YopM antibody.
- YopM is strongly immunogenic in mice, producing a predominantly IgG1 response, but is not a protective antigen for inbred or outbred mice immunized actively with pure YopM.
- YopM is not a good candidate for a subunit vaccine designed to protect via the humoral immune response.
- A pilot study of the relative roles of CD8<sup>+</sup> and CD4<sup>+</sup> T cells in the response of naïve mice to plague found a greater role for CD8<sup>+</sup> than CD4<sup>+</sup> T cells. This finding indicates an unexpected early role for CD8<sup>+</sup> T cells in protection against plague and merits further study. It suggests that an intracellular niche is important for *Y. pestis* early during plague, a conclusion that runs counter to the current view that *Y. pestis* is mainly extracellularly located. This is important, because the niche of a pathogen during infection has a large role in determining which arm of the immune response will be effective in clearing the pathogen and in the strategies that will be most effective for vaccine design. Potentially, the CD8<sup>+</sup> T cell response could be manipulated to give a novel way to enhance protection of humans against plague.
- These studies completed the work proposed for Aim 1.

### Aim 2. Determine if thrombin-binding is necessary for YopM function in vivo.

- Two *Y. pestis* mutants that made YopM proteins that interacted with thrombin normally according to the functional assay of inhibition of platelet aggregation were as avirulent as a YopM<sup>-</sup> *Y. pestis* strain, indicating that thrombin-binding is irrelevant to YopM's function in vivo.
- These studies completed the work proposed for Aim 2.



Aim 3. Determine the fate of YopM when *Y. pestis* interacts with phagocytic cells.

- Most of YopM is targeted into the cytosol of epithelial or phagocytic cells when *Y. pestis* adheres to them.
- If *Y. pestis* is phagocytosed, then the yersiniae do not target YopM or YopE into the eucaryotic cell cytosol.
- Within the eucaryotic cell, YopM interacts with the vesicular trafficking system.
- YopM enters the nucleus of the eucaryotic cell, a finding that potentially could mean that YopM's mechanism of action involves manipulating host gene expression.
- These studies completed the work proposed for Aim 3.

References

1. Straley, S. C., E. Skrzypek, G.V. Plano, and J.B. Bliska. 1993. Yops of *Yersinia* spp. pathogenic for humans. *Infect. Immun.* **61**: 3105-3110.
2. Leung, K.Y., B.S. Reisner, and S. C. Straley. 1990. YopM inhibits platelet aggregation and is necessary for virulence of *Yersinia pestis* in mice. *Infect. Immun.* **58**: 3262-3271.
3. Reisner, B.S., and S. C. Straley. 1992. *Yersinia pestis* YopM: thrombin binding and overexpression. *Infect. Immun.* **60**: 5242-5252.
4. Fenton, J.W. II. 1988. Regulation of thrombin generation and functions. *Sem. Thromb. Hem.* **14**: 234-240.
5. Plano, G.V., and S. C. Straley. 1995. Mutations in *yscC*, *yscD*, and *yscG* prevent high-level expression and secretion of V antigen and Yops in *Yersinia pestis*. *J. Bacteriol.* **177**:3843-3854.
6. Reed, L. J., and H. Muench. 1938. A simple method for estimating fifty percent endpoints. *Am. J. Hyg.* **27**:493-497.
7. Hansen, T. H., and D. H. Sachs. 1989. Chapter 16, the major histocompatibility complex. In: W. E. Paul, (ed.), *Fundamental Immunology*. Raven Press, New York.
8. Motin, V.L., R. Nakajima, G.B. Smirnow, and R.R. Brubaker. 1994. Passive immunity to Yersiniae mediated by anti-recombinant V

- antigen and protein A-V antigen fusion peptide. *Infect. Immun.* **62**:4192-4201.
9. Williams, J.E. and D.C. Cavanaugh. 1979. Measuring the efficacy of vaccination in affording protection against plague. *Bull. W.H.O.* **57**:309-313.
  10. Bahmanyar, M., and D.C. Cavanaugh. 1976. Plague manual. Ch. V. Serological methods. W.H.O., Geneva.
  11. Miller, J. H. 1972. Experiments in molecular genetics, p. 433. Cold Spring Harbor Laboratory, Cold Spring Harbor, NY.
  12. Nakajima, R., V.L. Motin, and R.R. Brubaker. 1995. Suppression of cytokines in mice by Protein A-V antigen fusion peptide and restoration of synthesis by active immunization. *Infect. Immun.* **63**:3021-3129.
  13. Leary, S.E.C., E. D. Williamson, K.F. Griffin, P. Russell, S. M. Eley, and R.W. Titball. 1995. Active immunization with recombinant V antigen from *Yersinia pestis* protects mice against plague. *Infect. Immun.* **63**:2854-2858.
  14. Anderson, G.W., S.E.C. Leary, E.D. Williamson, R.W. Titball, W.L. Welkos, P.L. Worsham, and A.M. Friedlander. 1996. Recombinant V antigen protects mice against pneumonic and bubonic plague caused by F1-capsule-positive and -negative strains of *Yersinia pestis*. *Infect. Immun.* **64**:4580-4585.
  15. Boland, A., M. -P. Sory, M. Iriarte, C. Kerbourn, P. Wattiau, and G. R. Cornelis. 1996. Status of YopM and YopN in the *Yersinia* Yop virulon: YopM of *Y. enterocolitica* is internalized inside the cytosol of PU5-1.8 macrophages by the YopB,D,N delivery apparatus. *EMBO J.* in press.
  16. Nemeth, J. and S.C. Straley. 1997. Effect of *Yersinia pestis* YopM on Experimental plague. *Infect. Immun.* **65**:924-930.
  17. Holmstrom, A., J. Pettersson, R. Rosqvist, S. Hakansson, F. Tafazoli, M. Fallman, K.-E. Magnusson, H. Wolf-Watz, and A. Forsberg. 1997. YopK of *Yersinia pseudotuberculosis* controls translocation of Yop effectors across the eucaryotic cell membrane. *Mol. Microbiol.* **24**:73-91.
  18. Leung, K.Y., and S. C. Straley. 1989. The *yopM* gene of *Yersinia pestis* encodes a released protein having homology with the human platelet surface protein GPIb $\alpha$ . *J. Bacteriol.* **171**:4623-4632.
  19. Kobe, B. and J. Deisenhofer. 1994. The leucine-rich repeat: a versatile binding motif. *Trends in Biochem. Sci.* **19**: 415-421.

20. R.D. Kobe, B. and J. Deisenhofer. 1995. A structural basis of the interactions between leucine-rich repeats and protein ligands. *Nature (London)*. **374**: 183-186.
21. Shapiro, R., J. F. Riordan, and B.L. Vallee. 1995. LRRning the Rite of springs. *Structural Biol.* **2**: 350-354.
22. Fenton, J. W. Thrombin interactions with hirudin. 1989. *Sem. Throm. Hem.* **15**: 265-268.
23. Stubbs, M., and W. Bode. 1995. The clot thickens: clue provided by thrombin structure. *Trends in Biochem. Sci.* **1**: 23-28.
24. Bode, W., and M. T. Stubbs. 1993. Spatial structure of thrombin as a guide to its multiple sites of interaction. *Sem. Throm. Hem.* **19**: 321-333.
25. Karshkov, A., and W. Bode. 1993. Electrostatic properties of thrombin: Importance for structural stabilization and ligand binding. *Sem. Throm. Hem.* **19**: 334-343.
26. Rydel, T.J. and A. Tulinsky. 1991. Refined structure of the hirudin-thrombin complex. *J. Mol. Biol.* **221**: 583-601.
27. Stone, S. R., P. J. Braun, and Hofsteenge. 1987. Identification of regions of  $\alpha$ -thrombin involved in its interaction with hirudin. *Biochemistry*. **26**: 4617-4624.
28. Skraypczak-Jankun, E., V. E. Carperos, K. G. Ravichandran, A. Tulinsky, M. Westbrook, and J. Maraganore. 1991. Structure of the hirugen and hirulog 1 complexes of  $\alpha$ -thrombin. *J. Mol. Biol.* **221**: 1379-1393.
29. Mathews, I. I., K. P. Padmanabhan, V. Ganesh, and A. Tulinsky. 1994. Crystallographic structures of thrombin complexed with thrombin receptor peptides: existence of expected and novel binding modes. *Biochemistry*. **33**: 3266-3279.
30. Fenton, J. W. 1989. Thrombin interactions with hirudin. *Sem. Throm. Hem.* **15**: 265-268.
31. Landschulz, W.H., P.F. Johnson, and S.L. McKnight. 1988. The leucine zipper: a hypothetical structure common to a new class of DNA binding proteins. *Science* **240**: 1759-1764.
32. Perry, R.D., J.D. Fetherston, S.C. Straley, D. Rose, and F. Blattner. 1998. Complete sequence of the low- $\text{Ca}^{2+}$  response plasmid of *Yersinia pestis* KIM. In preparation.
33. Skrzypek, E., and S.C. Straley. 1996. Interaction between *Yersinia pestis* YopM protein and human  $\alpha$ -thrombin. *Thrombosis Res.* **84**: 33-43.

34. Riordan, J.F. and B.L. Vallee. 1972. Chapter 36. Reactions with N-ethyl maleimide and p-mercuribenzoate. **In Methods in Enzymology 25 (PartB):449-456**
35. Metcalf, W.W., W. Jiang, L.L. Daniels, S.-K. Kim, A. Haldimann, and B. Wanner. 1996. Conditionally replicative and conjugative plasmids carrying *lacZ* $\alpha$  for cloning, mutagenesis, and allele replacement in bacteria. *Plasmid* **35**:1-13).
36. Hanahan, D., J. Jessee, and F.R. Bloom. 1991. Plasmid transformation of *Escherichia coli* and other bacteria. *Methods Enzymol.* **204**:63-113.
37. Perry, R.D., M. Pendrak, and P. Schuetze. 1990. Identification and cloning of a hemin storage locus involved in the pigmentation phenotype of *Yersinia pestis*. *J. Bacteriol.* **172**:5929-5937.
38. Bochner, B.R., H. Huang, G.L. Schieven, and B.N. Ames. 1980. Positive selection for loss of tetracycline resistance. *J. Bacteriol.* **143**:926-933.
39. Rosenshine, I., S. Ruschkowski, and B.B. Finlay. 1994. Inhibitors of cytoskeletal function and signal transduction to study bacterial invasion. *Meth. Enzymol.* **236**: 467-476.
40. Klausner, R.D., J.G. Donaldson, and Lippincott-Schwartz. 1992. Brefeldin A: insights into the control of membrane traffic and organelle structure. *J. Cell Biol.* **116**: 1071-1080.
41. Lemichez, E., M. Bomsel, G. Devilliers, J. vanderSpek, J.R. Murphy, E.V. Lukianov, S. Olsnes, and P. Bocquet. 1997. Membrane translocation of diphtheria toxin fragment A exploits early to late endosome trafficking machinery. *Mol. Microbiol.* **23**: 445-447.
42. Sandvig, K., and S. Olsnes. 1982. Entry of the toxic proteins abrin, modecin, ricin, and diphtheria toxin into cells. *J. Biol. Chem.* **257**: 7504-7513.
43. van Deurs, B., P.K. Holm, and K. Sandvig. 1996. Inhibition of the vacuolar H<sup>+</sup>-ATPase with bafilomycin reduces delivery of internalized molecules from mature multivesicular endosomes to lysosomes in Hep-2 cells. *Eur. J. Cell Biol.* **69**:343-350.
44. Adam, S. A., R. Sterne-Marr, and L. Gerace, 1991. In vitro nuclear protein import using permeabilized mammalian cells. *Meth. Cell Biol.* **35**: 469-482.
45. Diaz, R., and P.D. Stahl. 1989. Digitonin permeabilization procedures for the study of endosome acidification and function. *Meth. Cell Biol.* **31**: 25-43.

46. Sandvig, K. and B. van Deurs. 1996. Endocytosis, intracellular transport, and cytotoxic action of shiga Toxin and ricin. *Physiol. Rev.* **76**: 949-966.
47. Rothman, J. E. and F.T. Wieland. 1996. Protein sorting by transport vesicles. *Science* **272** : 227-234.
48. Lippincott-Schwartz, J. 1993. Bidirectional membrane traffic between the endoplasmic reticulum and the Golgi apparatus. *Trends Cell Biol.* **3**: 81-87.
49. Aniento, F., F. Gu, R.G. Parton, and J. Gruenberg. 1996. An endosomal  $\beta$ COP is involved in the pH-dependent formation of transport vesicles destined for late endosomes. *J. Cell. Biol.* **133**: 29-41.
50. Black, D. S., and J.B. Bliska. 1997. Identification of p130<sup>Cas</sup> as a substrate of *Yersinia* YopH (Yop51), a bacterial protein tyrosine phosphatase that translocate into mammalian cells and targets focal adhesions. *The EMBO J.* **16**: 2730-2744.
51. Lippincott-Schwartz, J., L. Yuan, C. Tipper, M. Amherdt, L. Orci, and R.D. Klausner. 1991. Brefeldin A's effects on endosomes, lysosomes, and the TGN suggest a general mechanism for regulating organelle structure and membrane traffic. *Cell* **67**:601-616.
52. Vale, R. D. 1987. Intracellular transport using microtubule-based motors. *Ann. Rev. Cell Biol.* **3**: 347-378.
53. Dingwall, C., and R.A. Laskey. 1991. Nuclear targeting sequences - a consensus?. *Trends Biochem. Sci.* **16**: 478-481.
54. Gorlich, D. and I.W. Mattaj. 1996. Nucleocytoplasmic transport. *Science*. **271**: 1513-1518.
55. Pollard, V. W., W.M. Michael, S. Nakielnny, M.C. Siomi, F. Wang, and G. Dreyfuss. 1996. A novel receptor-mediated nuclear protein import pathway. *Cell*. **86**: 985-994.
56. Pohlner, J., U. Langenberg, U. Wolk, S.C. Beck, and T.F. Meyer. 1995. Uptake and nuclear transport of *Neisseria* IgA1 protease-associated  $\alpha$  proteins in human cells. *Mol. Microbiol.* **17**: 1073-1083.
57. Howard, E., J.R. Zupan, V. Citovsky, and P.C. Zambryski. 1992. The VirD2 protein of *A. tumefaciens* contains a C-terminal bipartite nuclear localization signal: implications for nuclear uptake of DNA in plant cells. *Cell*. **68**: 109-118.

58. Van den Ackerveken, G., E. Marois, and U. Bonas. 1996. Recognition of the bacterial avirulence protein AvrBs3 occurs inside the host plant cell. *Cell* **87**: 1307-1316.
59. Straley, S.C., and P.A. Harmon. 1984. Growth in mouse peritoneal macrophages of *Yersinia pestis* lacking established virulence determinants. *Infect. Immun.* **45**:649-654.
60. Straley, S.C., and P.A. Harmon. 1984. *Yersinia pestis* grows within a phagolysosome in mouse peritoneal macrophages. *Infect. Immun.* **45**:655-659.
61. Straley, S.C., G.V. Plano, E. Skrzypek, P.L. Haddix, and K.A. Fields. 1993. Regulation by  $Ca^{2+}$  in the *Yersinia* low- $Ca^{2+}$  response. *Mol. Microbiol.* **8**:1005-1010.
62. Rosqvist, R., K.-E. Magnusson, and H. Wolf-Watz. 1994. Target cell contact triggers expression and polarized transfer of *Yersinia* YopE cytotoxin into mammalian cells. *EMBO J.* **13**:964-972.
63. Persson, C., R. Nordfelth, N. Holmström, S. Håkansson, R. Rosqvist, and H. Wolf-Watz. 1995. Cell-surface-bound *Yersinia* translocate the protein tyrosine phosphatase YopH by a polarized mechanism into the target cell. *Molec. Microbiol.* **18**:135-150.
64. Håkansson, S., E. E. Galyov, R. Rosqvist, and H. Wolf-Watz. 1996. The *Yersinia* YpkA Ser/Thr kinase is translocated and subsequently targeted to the inner surface of the HeLa cell plasma membrane. *Molec. Microbiol.* **20**:593-603.
65. Fallman, M., K. Andersson, S. Håkansson, K. -E. Magnusson, O. Stendahl, and H. Wolf-Watz. 1995. *Yersinia pseudotuberculosis* inhibits Fc receptor-mediated phagocytosis in J774 cells. *Infect. Immun.* **63**: 3117-3124.
66. Rosqvist, R., C. Forsberg, and H. Wolf-Watz. 1991. Intracellular targeting of the *Yersinia* YopE cytotoxin in mammalian cells induces actin macrofilament disruption. *Infect. Immun.* **59**: 4562-4569.
67. Cavanaugh, D.C. and R. Randall. 1959. The role of multiplication of *Pasteurella pestis* in mononuclear phagocytes in the pathogenesis of flea-borne plague. *J. Immunol.* **83**: 348-363.
68. Rosqvist, R., I. Bolin, and H. Wolf-Watz. 1988. Inhibition of phagocytosis in *Yersinia pseudotuberculosis*: a virulence plasmid-encoded ability involving the Yop2b protein. *Infect. Immun.* **56**: 2139-2143.

69. Balch, W.E., and J. E. Rothman. 1985. Characterization of protein transport between successive compartments of the Golgi apparatus: asymmetric properties of donor and acceptor activities in a cell-free system. *Arch. Biochem.* **240**:413-425.
70. Andersson, K., N. Carballeira, K.-E. Magnusson, C. Persson, O. Stendahl, H. Wolf-Watz, and M. Fallman. 1996. YopH of *Yersinia pseudotuberculosis* interrupts early phosphotyrosine signalling associated with phagocytosis. *Mol. Microbiol.* **20**:1057-1069.
71. Lindler, L.E., M.S. Klempner, and S. C. Straley. 1990. *Yersinia pestis* pH 6 antigen: genetic, biochemical and virulence characterization of a protein involved in the pathogenesis of bubonic plague. *Infect. Immun.*, **58**:2569-2577.
72. Skrzypek, E., and S. C. Straley. 1995. Differential effects of deletions in *lcrV* on secretion of V antigen, regulation of the low- $\text{Ca}^{2+}$  response, and virulence of *Yersinia pestis*. *J. Bacteriol.* **177**: 2530-2542.
73. Straley, S.C. and William S. Bowmer. 1986. Virulence genes regulated at the transcriptional level by  $\text{Ca}^{2+}$  in *Yersinia pestis* include structural genes for outer membrane proteins. *Infect. Immun.*, **51**: 445-454.
74. Wren, B.R., J. Henderson, and J.M. Ketley. 1994. A PCR-based strategy for the rapid construction of defined bacterial deletion mutants. *Biotechniques* **16**:994-996.
75. Mogensen, M.M., and J.B. Tucker. 1990. Taxol influences control of protofilament number at microtubule-nucleating sites in *Drosophila*. *J. Cell Sci.* **97**:101-107.

**Publications and abstracts resulting from the studies supported by Collaborative Agreement DAMD17-94-V-4013**

**Publications**

1. Skrzypek, E., and S.C. Straley. 1996. Interaction between *Yersinia pestis* YopM protein and human  $\alpha$ -thrombin. *Thrombosis Res.* **84**:33-43.
2. Nemeth, J. and S.C. Straley. 1997. Effect of *Yersinia pestis* YopM on Experimental plague. *Infect. Immun.* **65**:924-930.
3. Skrzypek, E., C. Cowan, and S.C. Straley. 1998. Translocation and trafficking of the *Yersinia pestis* YopM protein in HeLa cells. *Mol. Microbiol.* Submitted.

## Abstracts

1. Skrzypek, E., J. Nemeth, and S.C. Straley. Interaction between *Yersinia pestis* YopM protein and human  $\alpha$ -thrombin. National meeting of American Society for Microbiology, New Orleans, LA, May 19-23, 1996.
2. Skrzypek, E., and S.C. Straley. Translocation of *Yersinia pestis* YopM into eucaryotic cells. National meeting of American Society for Microbiology, Miami, FL, May 4-8, 1997.
3. Straley, S.C. Toxin special delivery in plague. The Hot Zone - 1997: Conference on Emerging Infectious Diseases, Lexington, KY, June 27-28, 1997.

## Personnel receiving pay from effort DAMD17-94-V-4013

### Research personnel

Susan C. Straley  
Ela Skrzypek  
Judith Nemeth

### Lab Aids (part-time assistants)

Michael Beiting  
Brent Payne  
Thomas Stoss  
James Rizzo